HHS Public Access

Author manuscript

Sci Immunol. Author manuscript; available in PMC 2020 July 07.

Published in final edited form as:

Sci Immunol. 2019 November 22; 4(41): . doi:10.1126/sciimmunol.aav5947.

Helios enhances the preferential differentiation of human fetal CD4+ naïve T cells into regulatory T cells.

Melissa S. F. Ng[1,2], **Theodore L. Roth**[1,3,4], **Ventura F. Mendoza**[5], **Alexander Marson**[3,4,6,7,8,9,10], **Trevor D. Burt**[3,5,11,12,*]

[1]Biomedical Sciences Graduate Program, University of California San Francisco (UCSF), San Francisco, CA 94143, USA.

[2]Singapore Immunology Network, Agency for Science, Technology and Research, Biopolis, 138648 Singapore.

[3]Department of Microbiology and Immunology, UCSF, San Francisco, CA 94143, USA.

[4]Diabetes Center, UCSF, CA 94143, San Francisco, USA.

[5]Eli and Edythe Broad Center of Regeneration Medicine and Stem Cell Research, UCSF, San Francisco, CA 94143, USA.

[6]Innovative Genomics Institute, University of California, Berkeley, CA 94720, USA.

[7]Department of Medicine, UCSF, San Francisco, CA 94143, USA.

[8]Chan Zuckerberg Biohub, San Francisco, CA 94158, USA.

[9]UCSF Helen Diller Family Comprehensive Cancer Center, UCSF, San Francisco, CA 94158, USA.

[10]Parker Institute for Cancer Immunotherapy, San Francisco, CA, USA.

[11]Department of Pediatrics, Division of Neonatology, UCSF, San Francisco, CA 94110, USA.

[12]Department of Pediatrics, Division of Neonatology, Duke University School of Medicine, Durham, NC, 27710, USA.#

Abstract

[*]To whom correspondence should be addressed. trevor.burt@duke.edu.
[#]Current Affiliation

Author Contributions: M.N. and T.D.B. conceptualized the project. M.N. designed and performed the experiments, and analyzed the data. V.F.M. aided in experiments. T.L.R. and A.M. provided advice and technical help on CRISPR-Cas9 editing experiments. M.N. and T.D.B. wrote the manuscript. All authors discussed the results and commented on the manuscript.

Competing Interests: A.M. is a co-founder of Spotlight Therapeutics. A.M. and T.L.R. are co-founders of Arsenal Biosciences. A.M. serves on the scientific advisory board of PACT Pharma, is an advisor to Trizell, and previously served as an advisor to Juno Therapeutics. A.M. has had speaking engagements with or done consulting for Amgen, ThermoFisher, Health Advances, Lonza, Bernstein, AbbVie, Genentech, Merck, Illumina, Arcus, Jackson Laboratories, Nanostring Technologies, GLG, RCM and Soteria. The Marson laboratory has received sponsored research support from Juno Therapeutics, Epinomics and Sanofi, and a gift from Gilead. The other authors declare that they have no competing interests.

Data and materials availability: ATACseq, H3K27ac ChIPseq, and all RNAseq raw and processed files are deposited in the Gene Expression Omnibus database under a superseries entry with the accession number GSE110472. The transcriptional and epigenetic gene lists defined in this manuscript are supplied in Supplementary Tables as described. All other data needed to evaluate the conclusions in the paper are present in the paper or the Supplementary Materials.

T cell receptor (TCR) stimulation and cytokine cues drive the differentiation of $CD4^+$ naïve T cells into effector T cell populations with distinct pro-inflammatory or regulatory functions. Unlike adult naïve T cells, human fetal naïve $CD4^+$ T cells preferentially differentiate into $FOXP3^+$ regulatory T (T_{reg}) cells upon TCR activation independent of exogenous cytokine signalling. This cell-intrinsic predisposition for T_{reg} differentiation is implicated in the generation of tolerance in utero; however, the underlying mechanisms remain largely unknown. Here, we identify epigenetic and transcriptional programs shared between fetal naive T and committed T_{reg} cells that are inactive in adult naive T cells, and show that fetal-derived induced T_{reg} (iT_{reg}) cells retain this transcriptional program. We show that a subset of T_{reg}-specific enhancers is accessible in fetal naive T cells, including two active super-enhancers at *Helios*. Helios is expressed in fetal naïve T cells but not in adult naïve T cells, and fetal iT_{reg} cells maintain Helios expression. CRISPR-Cas9 ablation of Helios in fetal naïve T cells impaired their differentiation into iT_{reg} cells upon TCR stimulation, reduced expression of immunosuppressive genes in fetal iT_{reg} cells such as *IL10*, and increased expression of pro-inflammatory genes including *IFNG*. Consequently, Helios knockout fetal iT_{reg} cells had reduced IL-10 and increased IFN-γ cytokine production. Together, our results reveal important roles for Helios in enhancing preferential fetal T_{reg} differentiation and fine-tuning eventual T_{reg} function. The T_{reg}-biased programs identified within fetal naive T cells could potentially be utilized to engineer enhanced iT_{reg} populations for adoptive cellular therapies.

One Sentence Summary:

Helios contributes to a transcriptional and epigenetic program in human fetal naïve T cells promoting T_{reg} differentiation.

Introduction

The adaptive immune system must generate immunotolerance in order to prevent or resolve pro-inflammatory responses that can cause host damage (1–3), while still permitting functional effector responses for host defense against pathogens (4, 5). A primary mechanism that achieves this flexibility is the capacity of $CD4^+$ naive T cells to differentiate into multiple specialized T helper (Th) subsets with either pro-inflammatory or immunosuppressive functions. The presence of polarizing cytokines within their immediate environment determines the eventual Th cell fate by triggering the expression and/or activation of master transcription factors that enact lineage specific transcriptional programs (6). For example, signaling by transforming growth factor-β (TGF-β) promotes the induction of FOXP3 (7–9), which is the master transcription factor required for the differentiation of naïve T cells into immunosuppressive regulatory T (T_{reg}) cells.

Mutations of the FOXP3 gene leading to the absence or dysfunction of T_{reg} cells result in the loss of T_{reg}-mediated immunotolerance, and trigger fatal, early onset multi-organ autoimmunity in both mice and humans (10–15). Autoimmunity resulting from the loss of $FOXP3^+$ T_{reg} cell-mediated tolerance in humans, defined as the IPEX (Immune dysregulation, polyendocrinopathy, enteropathy, X-linked) syndrome, can manifest within the fetus in utero and result in miscarriage, preterm birth, or death in childhood without hematopoietic stem cell transplant (16–20). The initiation of autoimmunity in IPEX coincides with the emergence of T cells in the second trimester of human development,

suggesting that T_{reg} cell-mediated peripheral tolerance is required during fetal development (21, 22). This is supported by the presence of an abundant population of fetal T_{reg} cells in the secondary lymphoid tissues, which comprise a larger percentage of the total $CD4^+$ T cell population compared to adults (23–25). However, thymic T_{reg} cell frequencies in fetal and infant thymus are not significantly different (24), indicating that increased thymic output is not responsible for the increased frequency of fetal T_{reg} cells. Fetal naive T cells, unlike their adult counterparts, preferentially differentiate into functional T_{reg} cells upon antigen stimulation, which include non-inherited maternal alloantigens (i.e. NIMAs) on maternal antigen-presenting cells (24). These findings imply that the abundance of fetal T_{reg} cells observed in fetal lymphoid tissues is due to peripheral conversion from naïve T cells. This propensity for T_{reg} differentiation is retained *in vitro*, as a high frequency of fetal naïve T cells differentiate into $FOXP3^+$ T_{reg} cells upon TCR activation even in the absence of exogenous TGF-β (26). The unique capability of fetal naïve T cells to initiate T_{reg} differentiation in the absence of exogenous TGF-β suggests that this ability is cell-intrinsic; however, the molecular mechanisms that underlie this predisposition are largely unknown.

Chromatin changes are also implicated in driving the final effector phenotype and function of differentiated T cells, defined by increases in chromatin accessibility of active lineage-specific genes, and the silencing of genes associated with other effector lineages (27, 28). In thymic and peripheral T_{reg} cells, permissive/active histone marks and DNA demethylation at T_{reg}-associated genes such as *IL2RA* (i.e., CD25), *CTLA4*, *IKZF2* (i.e., Helios), and *IKZF4* (i.e., Eos) (29, 30) must be acquired for commitment to and maintenance of the T_{reg} phenotype (29–32). This T_{reg}-chromatin landscape is acquired within developing thymic T_{reg} precursors before FOXP3 protein expression (30), indicating that a T_{reg}-specific epigenome may be responsible for initiating and promoting the expression of FOXP3. Additionally, other key genes associated with the T_{reg} epigenome, such as Helios, are expressed independently of FOXP3 expression (29, 30, 33), and can direct the partial acquisition of the T_{reg}-specific transcriptional signature when over-expressed in $FOXP3^-$ $CD4^+$ T cells (34). We therefore hypothesized that fetal naïve T cells might already possess a partial T_{reg}-specific epigenetic and transcriptional signature that predisposes them for differentiation towards the T_{reg} cell fate even without exogenous TGF-β signaling.

Here, we interrogated the transcriptional and chromatin landscape of fetal and adult naïve and T_{reg} cells, and discovered that components of the T_{reg} gene regulatory program are activated only in fetal naïve T cells. We then show that the partial T_{reg}-specific gene signature detected at steady state in fetal naïve T cells is retained only in fetal-derived, but not adult-derived induced T_{reg} (iT_{reg}) cells. We next identify two T_{reg}-specific super-enhancers (SEs) associated with the Helios locus that are active in fetal naïve T cells, in which we subsequently demonstrate the expression of Helios protein. Only iT_{reg} cells generated from fetal naïve T cells *in vitro* retained Helios expression and were characterized by repression of interleukin-2 (IL-2) production; neither of which were observed in adult iT_{reg} cells. CRISPR (clustered regular interspaced short palindromic repeats)-Cas9 (CRISPR-associated protein 9) mediated ablation of Helios in fetal naive T cells impaired their cell-intrinsic ability to differentiate into iT_{reg} cells in the absence of exogenous TGF-β. Analysis of the transcriptome in Helios knockout iT_{reg} cells revealed that Helios enhanced the upregulation of T_{reg}-specific genes (e.g., *IL10*) and mediated the repression of pro-

inflammatory genes involved in T effector differentiation and function (e.g., *IFNG*). Helios ablation in fetal iT$_{reg}$ cells resulted in decreased IL-10 production concurrent with increased IFN-γ and IL-2. Given that Helios has been previously characterized to be a gene specific to thymic T$_{reg}$ cells, our data reveal a new role for Helios as part of a pre-existing epigenetic and transcriptional program within human fetal naïve T cells that lowers the threshold for T$_{reg}$ differentiation and functional commitment. Taken together, we thus identify a TGF-β-independent mechanism unique to fetal naïve T cells that favors their differentiation into T$_{reg}$ cells, which may contribute insights into better engineering T$_{reg}$ cells *in vitro* from naïve T cells for use in immunotherapy.

Results

Human fetal naïve T cells express a partial T$_{reg}$ transcriptome.

Given that fetal naïve T cells preferentially differentiate into T$_{reg}$ cells upon TCR stimulation alone (26), we first asked if fetal naïve T cells shared elements of their transcriptome with T$_{reg}$ cells that could predispose them towards the T$_{reg}$ lineage. We performed RNA sequencing (RNAseq) on sorted fetal and adult CD4$^+$ naïve and T$_{reg}$ cells (see fig. S1 for sort gating strategy and purity confirmation). Principal component analysis (PCA) revealed that fetal and adult populations first segregated by cell origin (PC1, fetal or adult) before cell phenotype (PC2, naïve versus T$_{reg}$, Fig. 1A). PC2 scores for fetal naïve samples were intermediate to adult naïve and T$_{reg}$ samples (Fig. 1A), suggesting intermediate expression of T$_{reg}$-specific genes in fetal naïve T cells. In order to test this hypothesis, we first defined a T$_{reg}$-specific transcriptional signature by identifying genes differentially expressed in both fetal and adult T$_{reg}$ cells relative to adult naïve T cells based on a false discovery rate cut-off of FDR<0.05 and log 2 fold change (log$_2$FC) increase in expression of 1.5 (fig. S2, table S1). Fetal naïve T cells possessed intermediate upregulation/downregulation (Fig. 1B) across genes upregulated/downregulated in our T$_{reg}$-specific transcriptional signature. More specifically, relative to adult naïve T cells, fetal naïve T cells had 88 T$_{reg}$-upregulated and 42 T$_{reg}$-downregulated genes (Fig. 1C). We defined four different clusters within the T$_{reg}$-specific transcriptome (Fig. 1B, table S1) – two of which corresponded to all T$_{reg}$-upregulated genes (Cluster 1.1, 1.2), while the other two clusters contained all T$_{reg}$-downregulated genes (Cluster 1.3, 1.4). Within T$_{reg}$-upregulated genes, fetal naïve T cells did not express canonical T$_{reg}$ genes such as *FOXP3*, *IL2RA* and *CTLA-4* (Cluster 1.1, Fig. 1B). Instead, fetal naïve T cells had increased expression of T$_{reg}$-upregulated genes previously associated with T$_{reg}$ function such as *CCR4* (35, 36) and *KLF10* (37–39). Additionally, fetal naïve T cells had increased expression of the transcription factors *IKZF2* (Helios) (40–42) and *IKZF4* (Eos) (34, 43) (Cluster 1.2, Fig. 1B,1C) which are transcribed independently of FOXP3 expression in mice (29, 33, 44). Fetal naïve T cells and both the T$_{reg}$ cell populations shared similar downregulation of a subset of genes previously characterized as being downregulated in T$_{reg}$ cells such as *TSHZ2* and *SERPINB6* (45–47) (Cluster 1.3, Fig. 1B). In contrast, genes shared between fetal and adult naïve T cells included known genes contributing to the naïve T cell phenotype such as *TCF7* and *IL7R* (Cluster 1.4, Fig. 1B). Taken together, the presence of a partial T$_{reg}$-specific signature in fetal naïve T cells could thus potentiate T$_{reg}$ differentiation upon the receipt of

TCR signaling, consistent with the lowered threshold and greater propensity for these cells towards T_{reg} differentiation (24, 26).

Fetal-derived iT_{reg} cells maintain differential expression of the partial T_{reg}-specific transcriptome present in fetal naïve T cells.

We next asked if the partial T_{reg}-specific transcriptome detected in fetal naïve T cells would remain differentially expressed in fetal iT_{reg} cells, and whether adult iT_{reg} cells also acquire the T_{reg}-specific transcriptome after in vitro differentiation. To assess this, we performed RNAseq on fetal and adult iT_{reg} cells that underwent differentiation with TCR stimulation in media supplemented with IL-2 alone (IL-2-iT_{reg}) or additionally supplemented with TGF-β (TGF-β-iT_{reg}). PCA revealed that PC1 still segregated iT_{reg} populations by cell origin (fetal or adult), after which populations segregated by the stimulus received during differentiation (absence/presence of TGF-β, PC2, Figure 2A). This indicated that fetal-derived iT_{reg} cells were still transcriptionally different from adult-derived iT_{reg} cells, although the addition of TGF-β was sufficient to drive differential expression of a shared set of genes. We then evaluated all differentially expressed genes (FDR<0.05 and $\log_2$FC>1.5) across all iT_{reg} populations (Fig. 2B), and defined six clusters (table S2). Both fetal and adult TGF-β-iT_{reg} cells upregulated two gene clusters (Cluster 2.1 & 2.2, Fig. 2B, fig. S3A), and downregulated one gene cluster (Cluster 2.6, Fig. 2B, fig. S3A). T_{reg}-specific genes within Cluster 2.1 and 2.2 included genes known to be upregulated with TGF-β signaling such as *FOXP3* and *IKZF4* (48), as well genes potentially implicated in T_{reg} differentiation and function such as *SEMA4A* (49), *LTBP1*, *LTBP4* (50) and *LGALS3* (51, 52). However, only fetal IL-2- and TGF-β-iT_{reg} cells had increased expression of T_{reg}-specific genes that were upregulated in *ex vivo* fetal naïve T cells (Fig. 1C) such as *IKZF2*, *DUSP4*, *TOX* and *RGS1* (Cluster 2.3, Fig. 2B, fig. S3A). Decreased transcription of pro-inflammatory transcripts such as *IFNG*, *IL2*, *GZMB* and *IRF7* (Cluster 2.5, Fig. 2B, fig. S3A), and increased expression of genes involved in T_{reg} cell suppressive function such as *IL10* (Cluster 2.3, Fig. 2B) were only observed in fetal, but not adult, iT_{reg} cells. This suggested that, qualitatively, fetal iT_{reg} cells may have a transcriptome more reflective of *ex vivo* T_{reg} populations relative to adult iT_{reg} cells. We thus utilized Gene Set Enrichment Analysis (GSEA) to independently evaluate the transcriptomes of fetal or adult-derived iT_{reg} cells against published gene sets comparing T_{reg} and conventional T cell populations that also underwent TCR- and cytokine-stimulated activation *in vitro* (fig. S3B, table S3). In comparison to adult iT_{reg} cells, fetal iT_{reg} cells differentiated in both stimulation conditions had enrichment in genes upregulated in activated T_{reg} populations (Fig. 2B), and had enrichment of the partial T_{reg}-specific signature as defined by Cluster 1.2 and 1.3 (Fig. 1B, 2C, left, fig. S3C). Exogenous TGF-β signaling during T_{reg} differentiation resulted in the enrichment of Cluster 1.1 and depletion of Cluster 1.4 genes within fetal TGF-β-iT_{reg} but not adult TGF-β-iT_{reg} cells (Fig. 2C, right, fig. S3D). Our data thus show that differentiating fetal naïve T cells, independently of exogenous TGF-β, retain increased expression of the partial T_{reg}-specific transcriptional signature detected in *ex vivo* naïve T cells. Furthermore, the expression of these genes does not reach the same levels in adult iT_{reg} cells, suggesting that upstream mechanisms might be responsible for driving the transcriptional differences that favor T_{reg} differentiation in fetal naïve T cells.

Fetal iT$_{reg}$ cells have increased sensitivity to TGF-β signaling

In addition to increased expression of genes associated with T$_{reg}$ function, fetal IL-2-iT$_{reg}$ cells strongly upregulated a gene cluster which contained key genes associated with TGF-β sequestration and downstream signaling – including *SMAD1*, *TGFBR3*, *LRRC32* (54, 55) and *LIN28B* (26) (Cluster 2.4, Fig. 2B, fig. S4A). Expression of Lin28b protein in fetal naïve T cells contributes to increased expression of *TGFBR1, TGFBR3, SMAD2*, as well as increased phosphorylation of SMAD2/3 (26). GARP (*LRRC32*) is expressed highly on the cell surface of activated T$_{reg}$ cells and captures inactive TGF-β bound to the latency-associated peptide (LAP) (54, 56). This reservoir of cell-surface associated TGF-β is implicated in the maintenance of oral tolerance in mice (55), and in the induction of FOXP3 in naïve T cells co-cultured with GARP^{+}T$_{reg}$ cells (54). Here we demonstrate that fetal but not adult iT$_{reg}$ cells highly expressed *GARP* (fig. S4B) and *LAP* in a linear fashion (fig. S4C). Furthermore, fetal iT$_{reg}$ cells have increased transcription of *ITGB8* (Cluster 3, fig. 2B), the beta chain for the integrin $\alpha_v\beta_8$ which processes and releases bioactive TGF-β1 from LAP (55). Since fetal iT$_{reg}$ cells have increased cell surface-associated TGF-β and the machinery to mediate its potential release, we tested whether blockade of TGF-β1 with TGF-β-neutralizing antibodies resulted in decreased fetal T$_{reg}$ differentiation in response to TCR stimulation alone. As hypothesized, fetal T$_{reg}$ induction was blunted in the setting of TGF-β blockade (fig. S4D, E). However, fetal naïve T cells still retained an increased ability for T$_{reg}$ differentiation over adult naïve T cells, even when exogenous bioactive TGF-β was added (fig. S4D,E). Hence, although active TGF-β1 biogenesis may contribute to fetal iT$_{reg}$ differentiation in the absence of exogenous TGF-β, additional upstream mechanisms are responsible for driving enhanced fetal T$_{reg}$ differentiation *in vitro*.

Fetal naïve T cells share a partial epigenetic landscape with adult T$_{reg}$ cells

Given that fetal naïve T cells already express a partial T$_{reg}$-specific signature, we next assessed if we could also detect the presence of permissive epigenetic marks in fetal naïve T cells that could further drive the predisposition towards more robust T$_{reg}$ cell differentiation. In order to identify these chromatin features, we used Assay for Transposase-Accessible Chromatin followed by sequencing (ATACseq) and H3K27ac chromatin immunoprecipitation sequencing (ChIPseq) to compare regions of open and active chromatin in adult T$_{reg}$ cells relative to fetal and adult naïve T cells. Super-enhancers (SEs) and typical transcriptional enhancers (TEs) were classified using the ROSE algorithm (57, 58), and PCA was performed across enhancers identified in all samples. Cell origin (fetal versus adult) was the primary source of variance (PC1) in both ATACseq (Fig. 3A) and H3K27ac ChIPseq (Fig. 3B), and together with cell phenotype (naïve or T$_{reg}$), largely accounted for differences in the epigenome across all three populations. However, fetal naïve and adult T$_{reg}$ cell samples clustered together across the second source of variance (PC2) in both datasets (Fig. 3A,B). This suggested that, in addition to expression of a partial T$_{reg}$-specific transcriptome, fetal naïve T cells share a small subset of open and active T$_{reg}$-specific enhancers with adult T$_{reg}$ cells.

To address this possibility, we first independently defined enhancers differentially enriched for ATAC (fig. S5A) or H3K27ac (fig. S5B) signal in adult T$_{reg}$ cells relative to adult naïve T cells (FDR<0.05; expression fold change>1.5). Differentially enriched enhancers classified

as having both increased H3K27ac and ATAC signals in adult T_{reg} cells were termed T_{reg}-accessible enhancers (fig. S5C, table S4), while common enhancers were defined as having no difference in enrichment of both signals (fig. S5C). T_{reg}-inaccessible enhancers with decreased signals were similarly defined (table S5). We then assessed if any T_{reg}-accessible enhancers were enriched in fetal naïve T cells relative to adult naïve T cells. We found that fetal naive T cells had increased ATAC and H3K27ac signal at 38.8% (933/2405) and 4.6% (110/2405) of T_{reg}-accessible enhancers respectively (Fig. 3C, fig. S5D,E). These T_{reg}-accessible enhancers (table S4) were annotated to genes previously described to be part of the T_{reg}-specific epigenome, such as *IKZF2* (i.e., Helios), *IKZF4* (i.e., Eos) and *RXRA* (i.e., retinoic receptor RXR-alpha) (29, 30, 32). Similarly, 23.1% (426/1837) and 14% (258/1837) of T_{reg}-inaccessible enhancers also had decreased ATAC and H3K27ac signal, respectively, in fetal naive T cells (Fig. 3C, fig. S5D,E). Taken together, these data suggest that fetal naïve T cells at steady state are poised for T_{reg} differentiation by the acquisition of a partial T_{reg} epigenomic landscape characterized by increased chromatin accessibility at more than a third of all T_{reg}-accessible enhancers. Given that chromatin accessibility may precede H3K27ac deposition (59), acquisition of the T_{reg} epigenetic signature within fetal naïve T cells could occur in a stepwise fashion where full enhancer activation via H3K27 acetylation is acquired with the triggering of T_{reg} cell differentiation.

In light of this hypothesis, we evaluated transcription factor motif enrichment within all T_{reg}-accessible peaks shared between fetal naïve and committed adult T_{reg} cells (defined in a similar manner as TEs/SEs). Peak calls were utilized to minimize false positives stemming from the broadness of SE regions. Fetal naïve T cells had minimal enrichment of T_{reg}-accessible H3K27ac peaks, but had increased chromatin accessibility at a third of all T_{reg}-accessible ATAC peaks (fig. S6A). These shared T_{reg}-accessible peaks were enriched in binding motifs for the AP-1 complex (fig. S6B) and RUNX1 (fig. S6C, table S6), which are downstream of TCR signaling and play critical roles as transcriptional regulators of the FOXP3 locus and as co-factors for FOXP3 (60). We also detected a smaller subset of peaks that had enrichment of binding motifs for STAT5 (fig. S6D) and SMAD2/3 (fig. S6E). As such, increased chromatin accessibility could potentially synergize with enhancer activation and faster transcription of genes underlying STAT5 and SMAD2/3 binding sites with IL-2 and TGF-β signaling during fetal T_{reg} differentiation. Lastly, we examined differentially enriched T_{reg}-accessible peaks in fetal naïve T cells for the presence of FOXP3 binding sites previously identified in human T_{reg} cells(61). We show that only 5% (116/2213) of shared T_{reg}-accessible peaks with increased ATACseq signal have FOXP3 binding sites (fig. S6F). Taken together, we further illustrate that increased chromatin accessibility within fetal naïve T cells is largely poised to synergize with TCR and cytokine signaling cues, and to a smaller extent, direct binding of FOXP3, to drive their preferential differentiation into T_{reg} cells.

Fetal naïve T cells have increased open and active chromatin at two T_{reg}-accessible SEs associated with Helios

SEs are defined by high density regions of H3K27ac modifications, and they nucleate the assembly of transcription factors to drive expression of genes associated with cell lineage commitment (57, 58, 62). We saw that highly ranked SEs shared across fetal naïve, adult naïve, and adult T_{reg} samples corresponded to genes commonly associated with global T cell

development and function such as *BCL11B* (63) and *ETS1* (64) (fig. S7A, table S7). Because increased accessibility at T_{reg} SEs in murine thymic T_{reg} progenitors precedes FOXP3 upregulation and commitment to the T_{reg} lineage (30), we asked if increased accessibility at T_{reg}-accessible SEs in fetal naïve T cells could contribute to their priming towards T_{reg} differentiation. We identified 121 SEs within all T_{reg}-accessible enhancers, many of which were proximal to canonical T_{reg} genes including *FOXP3, IL2RA, CTLA4, TNFRSF4* (i.e., TNF receptor superfamily member 4) and *IKZF2* (Fig. 3D) as previously described in mice (30). Globally, fetal naïve T cells did not have greater accessible chromatin or H3K27ac enrichment at all T_{reg}-accessible SEs compared to adult naïve T cells (fig. S7B). This suggested that unlike thymic T_{reg} progenitors, fetal naive T cells might acquire active enhancer marks at the full T_{reg}-accessible SE signature only after T_{reg} differentiation. We next wondered if any SEs independently classified by ROSE, and preferentially enriched within fetal naïve T cells, were proximal to genes associated with T_{reg} accessible-SEs, since their presence would have been masked by the global analysis. Most genes associated with T_{reg} accessible-SEs did not have enrichment of H3K27ac signal that met the SE cut-off in both fetal and adult naïve T cells (Fig. 3E). One exception was the transcription factor *IKZF2* (i.e., Helios), which was unique to fetal naïve T cells (left, Fig. 3E), and previously identified to be one of the first T_{reg}-SEs to acquire permissive epigenetic marks in murine thymic T_{reg} progenitors (30). Adult naïve T cells had independent SE classification for one gene, *ZC3H12D* (right, Fig. 3E), which currently has no reported association with T_{reg} cell function.

Cell-specific SE regions are typically found proximal to genes encoding transcription factors that play key roles in cell identity by controlling the transcription of lineage-specific transcriptional programs (30, 57). We next focused our analysis on evaluating if any T_{reg}-accessible SEs defined within adult T_{reg} cells had increased enrichment of either ATAC or H3K27ac signal in fetal naive T cells (Fig. 3C), and were also associated with known transcription factors. Five T_{reg}-accessible SEs associated with four different transcription factors were identified to have increased ATAC signal (Fig. 3F), of which only two T_{reg}-accessible SEs were also differentially enriched for H3K27ac (Figure 3G). These active, H3K27ac-marked T_{reg}-accessible SEs were located in the intragenic and upstream regions within the Helios locus (Figure 4A), indicating that active expression of Helios might already be present in fetal naïve T cells. We further observed that Helios was a substantial contributor to the negative directionality of PC2 (Fig. 4B), which drove segregation of T_{reg} cells away from naïve T cell populations in our RNAseq dataset (Fig. 1A). Helios was also among the significant T_{reg}-upregulated genes with increased RNA transcription in fetal naïve T cells (Fig. 1C, Fig. 4C). Since enriched permissive epigenetic marks and transcription at the Helios gene locus regulate T_{reg} phenotype and function independent of FOXP3 expression in mice (29, 33, 65, 66), we further investigated Helios as a candidate contributing to the program of fetal T_{reg} differentiation.

Fetal naïve T cells have increased Helios protein expression at baseline.

Using flow cytometry staining, we show that fetal naïve T cells had higher Helios protein expression compared to adult naïve T cells (Fig. 4D,E). As previously described (40, 67), we identified $Helios^-$ and $Helios^+$ $FOXP3^+$ populations in adult T_{reg} cells (Fig. 4F). Fetal T_{reg}

cells were all uniformly Helios$^+$, which could indicate that retention of permissive epigenetic marks at Helios T_{reg}-accessible SEs may drive high Helios expression (Fig. 4F). An average of 60% of fetal naïve T cells were Helios$^+$, while adult naïve T cells did not express Helios (Fig. 4F&G). In comparison, we also examined the protein expression of two other T_{reg}-specific genes with increased transcription in fetal naïve T cells with differentially enriched ATAC signal, (CCR4; fig. S8C) or H3K27ac signal (Eos; fig. S8D). Relative to FOXP3 expression, CCR4 and Eos expression did not demonstrate a similar shift in expression within fetal naïve T cells from adult naïve T cells when compared to Helios (fig. S8E), which led us to focus on investigating the role of Helios expression in fetal T_{reg} cell differentiation.

The predisposition of fetal naïve T cells towards T_{reg} differentiation is not explained by increased incidence of CD31$^+$ cells in the naïve T cell population or increased proliferative ability.

Prior to further investigations into potential contributions of Helios to T_{reg} differentiation, we sought to address potential confounding factors in our analysis. Previous studies have demonstrated that CD31$^+$ population within the human naïve T cell population is enriched for recent thymic emigrants and have increased T_{reg} differentiation potential (68), making them potential precursors of T_{reg} cells in the periphery. We assessed if increased CD31$^+$ cell frequency was a contributor to increased T_{reg} differentiation in fetal naïve T cells, since the fraction of the CD31$^+$ population is highest at birth and decline with age (69). Unexpectedly, CD31$^+$ proportions were not different between adult and fetal naïve T cell populations (fig. S9A,B). Additionally, CD31$^+$ naïve T cells isolated from human peripheral blood do not demonstrate increased differentiation in the absence of exogenous TGF-β (67). We thus concluded that the predisposition towards T_{reg} differentiation that we observed within fetal naïve T cells was not attributed to differences in CD31$^+$ proportions.

We further observed that mean CD31 expression levels were reduced within fetal CD31$^+$ naïve T cells (fig. S9C). CD31 is downregulated with TCR signaling (69), and a subset of fetal CD4$^+$ T cells are CD69$^+$ and actively cycling (23). We therefore assessed the expression of CD69 and Ki67, a marker of active proliferation, relative to Helios expression in fetal naïve T cells. Neither fetal nor adult naïve T cells expressed CD69 (fig. S10A). However, as previously characterized (23), a subset of fetal naïve T cells are actively proliferating, while adult naïve T cells are mainly Ki67$^-$ (fig. S10B), thus possibly accounting for the reduced CD31 expression in fetal naïve T cells. The majority of the Ki67$^+$ population in fetal naïve T cells was also Helios$^+$ (fig. S10C), suggesting that Helios might regulate proliferation. However, with TCR stimulation, both adult and fetal naïve T cells upregulated Ki67 to a similar extent after 5 days (fig. S10D), indicating that Helios expression does not confer any selective proliferation advantage on fetal naïve T cells during T_{reg} differentiation that may account for their increased T_{reg} differentiation potential.

Fetal naïve T cells do not have increased demethylation at the FOXP3 T_{reg}-specific demethylated region (TSDR)

As Helios was first identified as a marker of thymic T_{reg} cells (40), we sought to rule out possible contamination of thymic T_{reg} cells by assessing demethylation of the TSDR at the

conserved non-coding sequence 2 (CNS2) region within the *FOXP3* gene in our sorted naïve T cell populations (fig. S1). We saw that as expected, only fetal and adult T_{reg} populations had complete TSDR demethylation, while both fetal and adult naïve T cells had a fully methylated TSDR (fig. S11A). This indicated that Helios expression within fetal naïve T cells was cell-intrinsic and not due to contamination with thymic T_{reg} cells.

Fetal naïve T cells upregulate and maintain Helios expression during iT_{reg} differentiation

Helios is expressed independently of FOXP3 expression (29, 33, 44) and can enhance the acquisition of a T_{reg}-transcriptional signature with the co-expression of FOXP3 (34). As such, Helios expression in fetal naïve T cells might allow them to bypass the need for TGF-β to initiate FOXP3 upregulation and underlie their preferential differentiation into T_{reg} cells. To assess this, we tracked Helios expression within fetal and adult naïve T cells during T_{reg} differentiation with IL-2 alone or with TGF-β added at 1, 3, or 5 days. As previously observed, a higher frequency of fetal naïve T cells differentiated into $CD25^{hi}FOXP3^{hi}$ iT_{reg} cells relative to adult naïve T cells either in the presence or absence of exogenous TGF-β (24, 25) (fig. S12A,B). Fetal naïve T cells highly upregulated and maintained Helios protein expression during iT_{reg} differentiation, whereas adult naïve T cells did not (fig. S12C,D). Concurrent upregulation of both FOXP3 and Helios was observed only in fetal iT_{reg} cells differentiated in both stimulation conditions; even as FOXP3 expression increased with TGF-β stimulation, Helios expression was not upregulated in adult iT_{reg} cells at any time point (Fig. 5A, B). Although Helios has been implicated as a marker of activation in proliferating cells (70), we show that both fetal and adult iT_{reg} cells upregulated Ki67 to the same extent, but only fetal iT_{reg} maintained upregulation of Helios (fig. S12E), thus excluding the probability that Helios upregulation in fetal iT_{reg} cells resulted from increased cell proliferation. We also excluded the possibility of thymic T_{reg} outgrowth leading to Helios expression within fetal iT_{reg} cells. As previously shown (71–73), we did not detect any TSDR demethylation for adult TGF-β-iT_{reg} populations (fig. S11A–C). Assessment of sorted fetal $FOXP3^-$, $FOXP3^+Helios^-$ and $FOXP3^+Helios^+$ IL-2- or TGF-β-iT_{reg} populations (fig. S11D,E) did not reveal TSDR demethylation in any fetal iT_{reg} populations (fig. S11A), thus suggesting that the increase in Helios expression happens *de novo* in fetal iT_{reg} cells.

The proportions of fetal IL-2-iT_{reg} cells generated across time tracked closely with proportions of adult TGF-β-iT_{reg} cells (fig. S12B), suggesting that Helios expression within fetal naïve T cells could enhance their preferential differentiation into T_{reg} cells independently of exogenous TGF-β. We further examined fetal $Helios^+$ and $Helios^-$ populations after T_{reg} differentiation and found that the majority of fetal iT_{reg} cells were within the $Helios^+$ population 24 hours after the initiation of T_{reg} induction (Fig. 5C). The increased frequency of iT_{reg} cells present within the $Helios^+$ over the $Helios^-$ population was maintained over time and in both stimulation conditions (Fig. 5D). $Helios^+$ cells also consistently had higher FOXP3 expression (Fig. 5E) relative to $Helios^-$ cells, suggesting that Helios expression could potentially drive increased FOXP3 expression in differentiating fetal naive T cells.

Helios knockout in fetal naïve T cells impairs their ability to preferentially differentiate into T_{reg} cells

Given the hypothesized role of Helios in enhancing FOXP3 upregulation during fetal T_{reg} cell differentiation, we predicted that reduced Helios expression in fetal naïve T cells would subsequently inhibit their cell-intrinsic propensity for T_{reg} differentiation. Using CRISPR-Cas9 mediated editing, we knocked out *Helios* with two independent guide RNAs (gRNAs) targeting different exons of the gene. Fetal naïve T cells were then assessed for T_{reg} induction post editing after differentiation in the presence or absence of exogenous TGF-β (Fig. 6A). We first confirmed that both gRNAs were able to successfully disrupt the Helios locus (fig. S13A–C), and observed specific reduction of Helios protein (Fig. 6B) in comparison to the non-targeting (NT) guide. Both gRNAs resulted in an average of 70% of fetal naïve T cells losing Helios expression (fig. S13D), and the reduction was maintained after 6 days of T_{reg} induction in both stimulation conditions (Fig. 6B,C). *Helios* knockout in stimulated fetal naïve T cells reduced subsequent T_{reg} differentiation in the absence of exogenous TGF-β compared to cells that received the NT guide (Fig. 6D,E), and the reduction in T_{reg} percentage correlated with the extent of knockout generated (fig. S14A). Adult naïve T cells nucleofected with the same guides were used as T_{reg} gating controls (fig. S13E). In contrast, Helios knockout had no effect on fetal iT_{reg} differentiation with addition of exogenous TGF-β (Fig. 6D, E, fig. S14B). This indicated that signaling via TGF-β compensated for the loss of Helios-driven T_{reg} differentiation, and that Helios and TGF-β may participate in shared signaling pathways. Our data show that Helios expression within fetal naive T cells plays a role in enhancing preferential T_{reg} differentiation specifically in the absence of exogenous TGF-β. This mechanism present within fetal naïve T cells could lower the threshold required for T_{reg} cell differentiation, thus potentially allowing for the default generation of peripheral T_{reg}-mediated tolerance upon antigen encounter during fetal development.

Helios suppresses IL-2 secretion in fetal iT_{reg} cells.

Helios maintains an anergic and non-proliferative state characteristic of the T_{reg} phenotype (74) by mediating the epigenetic silencing of the *IL2* locus in T_{reg} cells (75). In contrast to conventional T cells, T_{reg} cells have reduced IL-2 production upon TCR stimulation and depend heavily on paracrine IL-2 for their maintenance (76). Since Helios is highly expressed and maintained in fetal iT_{reg} cells, we investigated whether this led to a corresponding suppression of IL-2 production. As hypothesized, fetal iT_{reg} cells demonstrated less IL-2 production upon restimulation compared to adult iT_{reg} cells (fig. S15A), and suppression of IL-2 was observed regardless of iT_{reg} differentiation conditions (fig. S15B). When delineated on the basis of $Helios^{hi}$ and $Helios^{lo}$ expression (fig. S15C), $Helios^{hi}$ fetal iT_{reg} cells consistently had lower IL-2 production across both stimulation conditions (fig. S15D), indicating that high Helios expression may be associated with greater repression of the *IL2* locus. Helios knockout in fetal iT_{reg} cells then resulted in increased IL-2 production in IL-2-iT_{reg} cells (fig. S15E,F). Furthermore, Helios knockout TGF-β-iT_{reg} cells also produced more IL-2 upon restimulation when compared to the NT control (fig. S15E,F). This demonstrates that continued Helios expression in fetal naïve T cells not only enhances preferential T_{reg} differentiation, but also aids in the repression of IL-2 production in fetal iT_{reg} cells.

Helios knockout results in the downregulation of genes associated with T_{reg} differentiation and function and the concurrent upregulation of pro-inflammatory genes

Helios controls the expression of several key genes involved in T_{reg} suppressive function (77) including GARP. Helios knockout in fetal naïve T cells did not impact FOXP3 or CD25 expression (fig. S14C, D), but resulted in decreased CTLA-4 expression in fetal iT_{reg} cells (fig. S14E). Helios knockout also resulted in a trend towards downregulation of GARP and LAP on fetal iT_{reg} cells (fig. S14F,G). Since the impact of Helios knockout was variable across the conventional T_{reg} markers surveyed, and fetal iT_{reg} cells retain expression of a partial T_{reg}-specific transcriptional signature, we wondered whether transcriptional control of other T_{reg} genes by Helios could enhance the conversion of fetal naïve T cells into iT_{reg} cells as well as influence their subsequent function. As such, we further assessed the impact of Helios ablation on the fetal iT_{reg} transcriptome by RNA sequencing. CRISPR-Cas9 editing was carried out in fetal naïve T cells with Helios gRNA1 ($Helios^{KO}$) or the NT control ($Helios^{WT}$) before T_{reg} differentiation was induced in the absence or presence of TGF-β (fig. S16A).

PCA revealed that $Helios^{KO}$ and $Helios^{WT}$ iT_{reg} cells segregated largely according to whether differentiation occurred in the presence or absence of TGF-β (PC1, fig. S16B). This was not unexpected, since TGF-β signaling is responsible for the upregulation and repression of a significant subset of T_{reg}-specific genes (Fig. 2B–D). We also detected a small but distinct segregation of $Helios^{KO}$ from $Helios^{WT}$ cells, with PC2 mainly segregating $Helios^{KO}$ and $Helios^{WT}$ IL-2-iT_{reg} cells (fig. S15C), while PC3 mainly distinguished $Helios^{KO}$ and $Helios^{WT}$ TGF-β-iT_{reg} cells (fig. S15D). As full knockout of Helios expression is not achieved within the total iT_{reg} population with an average of 30% of all cells still retaining Helios expression (fig. S16A), we expected that this would result in a lowered signal-to-noise ratio. We thus utilized a more generous cutoff, where genes with at least a 10% change in expression (FC>1.1, FDR<0.05) were defined to be differentially expressed (fig. S15E,F).

Given that TGF-β signaling is able to compensate for the defect in T_{reg} induction in $Helios^{KO}$ iT_{reg} cells (Fig. 6D,E), we decided to dissect possible pathways controlled by Helios and TGF-β signaling in parallel (Fig. 7A). We first identified differentially expressed genes within both stimulation conditions that would normally be upregulated with TGF-β signaling within $Helios^{WT}$ iT_{reg} cells but were downregulated in $Helios^{KO}$ cells. This allowed us to detect genes whose expression was potentially enhanced by Helios in a complementary fashion – these genes would show decreased expression in $Helios^{KO}$ IL-2-iT_{reg} cells, but due to compensation with TGF-β signaling, would have no change in expression in $Helios^{KO}$ TGF-β-iT_{reg} cells compared to $Helios^{WT}$ controls (Fig. 7B,C). Similar cutoffs were used to define genes potentially suppressed by Helios in parallel, which would be upregulated in $Helios^{KO}$ IL-2-iT_{reg} cells. We identified 199 downregulated and 161 upregulated genes within $Helios^{KO}$ IL-2-iT_{reg} cells that were not differentially expressed in TGF-β-iT_{reg} cells (Fig. 7B). $Helios^{KO}$ IL-2-iT_{reg} cells had reduced expression of T_{reg}-specific genes previously identified to be exclusively upregulated in fetal iT_{reg} cells such as *DUSP4*, *IL10* and *ITGAE* (CD103) (Fig. 7B, table S10). Concurrently, $Helios^{KO}$ IL-2-iT_{reg} cells upregulated several chemokine and tumor necrosis factor (TNF) superfamily

genes (Fig. 7B, table S10), indicating that Helios may enhance the expression of a subset of T_{reg} genes while simultaneously reducing expression of pro-inflammatory genes associated with effector function in the absence of TGF-β signaling.

Additionally, synergy between Helios and TGF-β signaling might occur, thus amplifying the expression of T_{reg}-specific genes in an additive manner (Fig.7A). We thus assessed genes that had decreased expression specifically in Helios^{KO} TGF-β-iT_{reg} cells (Fig. 7C). Loss of Helios expression resulted in the downregulation of 351 genes in TGF-β-iT_{reg} cells (Fig. 7C), including *SEMA4*, *PTGS1* and *RTKN*, previously identified in the TGF-β-iT_{reg} gene signature (Cluster 2.2, Fig. 2B), as well as *TOX2* and *RGS1*, which are upregulated in fetal but not adult iT_{reg} cells (Cluster 2.3, Fig. 2B, table S10). Conversely, Helios^{KO} TGF-β-iT_{reg} cells had upregulation of 251 genes; these comprised chemokine receptor genes, as well as transcription factors involved with Th1, Th2 and Th17 cell differentiation and function such as *PRDM1* (Blimp1)(78), *GATA3* (79), *IKZF1* (Ikaros) (80, 81), and *MAF* (c-MAF) (82) (Fig. 7C). These data suggest that Helios performs both parallel and additive roles in enhancing the upregulation of genes associated with the T_{reg} transcriptional signature and repressing genes that might drive differentiation towards other effector T cell pathways during T_{reg} differentiation.

Lastly, we identified genes that were either upregulated or downregulated in Helios^{KO} iT_{reg} cells across both induction conditions, implicating possible transcriptional control by Helios independent of TGF-β signaling during T_{reg} differentiation. 200 genes were downregulated in Helios^{KO} iT_{reg} cells, including genes related to T_{reg} phenotype and function such as *CTLA4* and *LTBP4* (Fig. 7D,E). Although we did not observe reduced protein expression of FOXP3 in Helios^{KO} iT_{reg} cells at Day 6 of differentiation (Fig. S14C), we observed decreased FOXP3 transcription across both iT_{reg} populations, suggesting that additional post-transcriptional mechanisms probably regulate FOXP3 expression downstream of Helios. Helios^{KO} iT_{reg} cells also had reduced expression of *NFATC4* (NFAT3) and *PPARA* (PPARα) transcription factors which regulate the repression of pro-inflammatory cytokines such as IL-2, IFN-γ and TNF-α (83, 84), as well as the histone H3K27 demethylase *KDM6B* (JMJD3), which suppresses Th2 and Th17 programs (85) (Fig. 7D,E). Loss of Helios expression also led to the upregulation of 88 genes, including genes attributed to pro-inflammatory effector T cell function such as *IFNG* (Fig. 7D,E). Taken together, we propose that Helios could potentially play a role in enhancing fetal T_{reg} differentiation through the transcriptional regulation of a key subset of genes that restrict differentiation towards effector T cell helper phenotypes while favoring differentiation towards the T_{reg} cell fate.

Helios knockout fetal iT_{reg} cells have decreased IL-10 and increased IFN-γ production

The regulation of cytokine production in T_{reg} cells is important for their suppressive ability; T_{reg} cells must repress secretion of pro-inflammatory cytokines such as IFN-γ while maintaining production of immunosuppressive cytokines such as IL-10 (86). Given that we detected decreased IL-10 expression in Helios^{KO} IL-2-iT_{reg} cells (Fig. 7B), with a corresponding increase in IFN-γ transcription in both Helios^{KO} iT_{reg} populations (Fig. 7D,E), we next validated these observations by assessing IL-10 and IFN-γ in supernatant during iT_{reg} differentiation. We first confirmed that only fetal iT_{reg} cells produced IL-10

during iT_{reg} differentiation in the absence of TGF-β (Figure. 8A), as observed in our transcriptomic analysis of fetal and adult iT_{reg} cells (Fig. 2B). This is further augmented by exogenous TGF-β (Fig. 8A), which may be due to an increased frequency of T_{reg} cell differentiation (Fig. S5B). Fetal iT_{reg} cells also produced less IFN-γ than adult iT_{reg} generated in both stimulation conditions (Fig. 8B). Lastly, both fetal iT_{reg} cell populations had a greater ratio of IL-10 produced over IFN-γ compared to their adult counterparts, and this effect was enhanced in TGF-β-iT_{reg} cells (Figure 8C). Ablation of Helios with either gRNA1 or 2 then resulted in a reduction of IL-10 produced in $Helios^{KO}$ IL-2-iT_{reg} cells (Fig. 8D). We observed a small but sustained decrease in IL-10 across $Helios^{KO}$ TGF-β-iT_{reg} cells that received gRNA1 but did not detect this decrease in gRNA2 (Fig. 8D), which reflected our RNA sequencing results showing a minimal decrease in IL-10 in gRNA1 treated TGF-β-iT_{reg} that did not meet fold change cutoffs (fig. S16G). This is consistent with our prediction that TGF-β signaling can compensate for Helios knockout to upregulate *IL10* transcription within $Helios^{KO}$ TGF-β-iT_{reg} cells (Figure 7A). *Helios* knockout resulted in increased IFN-γ production in $Helios^{KO}$ TGF-β-iT_{reg} cells, but the effect was less obvious in IL-2-iT_{reg} cells (Fig. 8E). However, across all differentiation conditions, $Helios^{KO}$ iT_{reg} cells had a decrease in their IL-10 to IFN-γ ratio (Fig. 8F), especially in TGF-β-iT_{reg} cells. Overall, this suggests an potential role for Helios in regulating the balance of cytokine output from fetal iT_{reg} cells, which could help prevent pro-inflammatory responses that can be detrimental *in utero*.

Discussion

The predisposition of human fetal naïve T cells towards T_{reg} cell differentiation presents an opportunity to identify potential underlying cell-intrinsic factors that not only enhance our understanding of T_{reg} differentiation and function, but also may ultimately be manipulated to improve *in vitro* iT_{reg} cell generation for cell-based immunotherapies. We show here that fetal naïve T cells possess a partial T_{reg}-specific transcriptome and epigenome, and that only fetal-derived iT_{reg} cells retain expression of this transcriptome upon differentiation *in vitro*. Fetal naïve T cells had increased chromatin accessibility at approximately a third of all defined T_{reg}-accessible enhancers, but only a small percentage were marked by H3K27ac, including two SEs associated with Helios. This suggests that many T_{reg}-specific enhancers are held in a poised (i.e., accessible), but not active, state in quiescent fetal naïve T cells. As such, the full acquisition of the T_{reg}-specific epigenetic, and subsequently, transcriptional signature might only occur upon TCR activation and/or cytokine signaling which triggers the final commitment to the T_{reg} cell fate. These data thus implicate a broad landscape of T_{reg}-poised chromatin in fetal naïve T cells that contribute to their propensity for T_{reg} differentiation. It is likely that there is also a contribution of additional histone marks to the overall chromatin landscape. For example, since Helios interacts with other histone-modifying proteins such as the NuRD co-repressor complex (87, 88), sequencing of additional histone marks such as the repressive H3K27me3 mark would allow us to assess possible repression of genes associated with other effector lineages. Future experiments that identify Helios binding sites by Helios ChIPseq within fetal naïve or iT_{reg} populations will be critical to determine if Helios is required for the acquisition and/or maintenance of active or suppressive epigenetic marks at key T_{reg}-specific genes. These further analyses would

reveal a more complete understanding of the contribution of Helios to the fetal epigenome and how it contributes to the overall T_{reg} cell differentiation phenotype.

Our group and others have shown that the human fetal immune system is skewed towards tolerance by the presence of a large T_{reg} cell population (24, 25) which is likely derived from preferential conversion of fetal naive T cells into T_{reg} cells upon antigen encounter (26). Here, we show that Helios enhances the preferential differentiation and phenotypic commitment of fetal naïve T cells towards the T_{reg} cell fate. Ablation of Helios expression in fetal naïve T cells impaired their cell-intrinsic predisposition for iT_{reg} differentiation, and reduction in T_{reg} proportions were correlated with the extent of Helios knockout. Although the addition of exogenous TGF-β compensates for loss of Helios during T_{reg} generation, the resulting transcriptional landscape in $Helios^{KO}$ fetal TGF-β-iT_{reg} cells was still impacted. Our results suggest that Helios-mediated transcriptional regulation may potentially play a dual role in fetal T_{reg} differentiation – first, by enhancing T_{reg} differentiation through upregulation of a set of T_{reg}-specific genes even in the absence of TGF-β, and second, by repressing pro-inflammatory genes and genes that mediate differentiation towards other effector T cell subsets. This is consistent with the established role of Helios in restraining effector Th1 and Th17 cell programs within committed T_{reg} cells in mice (41, 42). While global transcriptional differences observed between $Helios^{KO}$ and $Helios^{WT}$ iT_{reg} cells were modest, we propose that the observed enhancement of fetal iT_{reg} differentiation is the result of cumulative effects of upregulation or downregulation of genes transcriptionally controlled by Helios. Validation of other gene candidates identified here would further clarify the extent of Helios transcriptional control on the human fetal iT_{reg} differentiation. Lastly, we demonstrate that Helios expression in fetal iT_{reg} cells has functional consequences, as the loss of Helios increased the ratio of pro-inflammatory (IFN-γ) over anti-inflammatory (IL-10) cytokines by these cells. This is consistent with previous observations that Helios deficiency in mouse T_{reg} cells *in vivo* does not result in overt distortions in FOXP3 expression or T_{reg} proportions at steady state (89), but rather in the loss of immunosuppressive ability and the manifestation of autoimmunity in later life or in response to inflammatory insults (41, 42). Regulation of cytokine and other pro-inflammatory genes by Helios could then potentially play a role in maintaining the functional stability of fetal iT_{reg} cells *in utero* to prevent potentially harmful pro-inflammatory responses.

Given the nature of this study, and the exclusive use of primary human cells, there are important limitations to acknowledge in its interpretation. We primarily compared T cells isolated from fetal spleen and adult peripheral blood for our studies, due to practical difficulties in obtaining adult splenic tissue and fetal peripheral blood. While we cannot fully rule out immunological differences associated with tissue residence, we have taken steps to reduce confounders resulting from this factor by deriving the epigenetic T_{reg} signature from comparisons of adult naïve and adult T_{reg} cells, thus ensuring that only the T_{reg} signature was the main point of comparison between adult and fetal naive T cells. We were able to additionally rule out contributions from age specific differences by selecting genes shared between adult and fetal T_{reg} cells in our RNAseq analysis to ensure that only genes truly contributing to the T_{reg} cell phenotype were included. Gestational age, and on some occasions when it could be determined, sex, were the only demographics available for fetal cells. Hence, we were unable to fully rule out any other potential confounders or stratify our

samples accordingly. Furthermore, technical variation due to the kinetics of CRISPR-Cas9 editing, together with the inherent biological variability in primary human samples manifested in the high sample variability that we observed within our editing experiments. We also observed heterogeneity in Helios expression at steady state in fetal naïve T cells, as well as the extent of Helios upregulation from sample to sample, which could contribute to differences in sensitivity to Helios disruption and subsequent T_{reg} differentiation. While we focused here on Helios, additional transcription factors unregulated in fetal naive T cells, such as Eos (IKZF4), could also play complementary or compensatory roles in fetal iT_{reg} differentiation. We envision that future work will aim to utilize single cell RNA or ATAC sequencing techniques to separate and identify fetal naïve T cell populations that will explain the observed biological heterogeneity. This will allow us to potentially identify subsets that have greater predisposition towards T_{reg} differentiation, and further characterized the underlying factors leading to this phenotype.

Our work here suggests a key role for Helios in establishing early life peripheral tolerance in humans, and there are some indications to support this hypothesis from studies in neonatal mice. Notably, when Helios$^{-/-}$ mice were first generated, the authors reported the presence of significant fatality in the first two weeks of neonatal life, and a 100% fatality was observed with subsequent crosses to achieve a full B6 background (89). This timing coincides with the emergence and migration of functional T cells into the secondary lymphoid organs within the neonatal mouse, and is developmentally equivalent to when T cells emerge during the second trimester in humans (21). Furthermore in mice, thymic T_{reg} cell populations generated in an early window from birth to 10 days later are qualitatively different from those generated later in life (90), indicating that T_{reg} cell populations generated in early life are indispensable to the maintenance of lifelong tolerance. However, these studies did not examine the potential contributions of peripheral T_{reg} differentiation from naïve T cells, which is likely an important factor contributing to the dominant tendency toward tolerance observed in the human fetus. This is particularly significant since there is an increased frequency of rapidly proliferating $CD4^+$ and $CD8^+CD25^-$ human fetal T cell populations (23) potentially bearing autoreactive TCRs that have escaped thymic deletion as observed in neonatal mice (91). In light of our data presented here, we thus speculate that Helios plays a previously unappreciated role in the generation of peripheral T_{reg} cells in this critical period in early human fetal development where the need for peripheral tolerance is perhaps the most acute.

In vitro human T_{reg} cell differentiation from naïve T cells for therapeutic purposes has encountered significant roadblocks due to difficulties in generating pure populations of T_{reg} cells that maintain a stable phenotype over time (71–73). Previous studies have show that Helios$^+$, but not Helios$^-$ *ex vivo* T_{reg} cells retain a more highly demethylated TSDR when expanded *in vitro* (92, 93). We did not observe TSDR demethylation in Helios$^+$ fetal iT_{reg} cells, likely reflecting the inability of *in vitro* differentiation to capture the conditions or environmental factors that trigger TSDR demethylation. Regardless, we demonstrate that fetal iT_{reg} cells have greater phenotypic resemblance to *ex vivo* T_{reg} cells in that they retain expression of Helios, have diminished IL-2 production upon restimulation, and produce IL-10 upon T_{reg} differentiation. These attributes are commonly associated with the T_{reg} cell phenotype, but are not acquired in adult human iT_{reg} cell populations. Lastly, our data shows

that Helios enhances the expression of genes in parallel with, in addition to, and independently of TGF-β signaling, which favor T_{reg} over helper T effector commitment. This may represent a mechanism by which Helios maintains stable T_{reg} function and identity *in vivo* (41, 42, 67, 75, 77). Additional studies are thus required to assess this possibility, particularly in pro-inflammatory environments, and whether manipulation of Helios expression within adult naïve T cells can recapture this effect. Further identification of upstream factors in addition to Helios that contribute to the acquisition of the permissive enhancer landscape in fetal naïve T cells will likely provide important deeper insight into their predisposition toward T_{reg} differentiation. These findings may then ultimately inform strategies for the generation of stable iT_{reg} cells for use in for immunotherapy to establish tolerance in autoimmunity and transplantation.

Materials and Methods

Study design

The objective of this study was to determine the molecular mechanisms that underlie preferential T_{reg} cell differentiation in human fetal naïve T cells. As such, primary human $CD4^+$ naïve T and T_{reg} cells from fetal spleen and adult peripheral blood mononuclear cells (PBMCs) were the primary cell sources used for this study. Transcriptional and epigenetic profiling was carried out utilizing RNAseq, H3K27ac ChIPseq and ATACseq. Flow cytometry was utilized to confirm observations from sequencing datasets, to validate expression levels at baseline, and to assess the activation and subsequent differentiation of fetal and adult naïve T cells *in vitro*. CRISPR-Cas9 mediated knockout was used to confirm the results of the observational studies. The sample size (n = 2–6 per experiment) for the sequencing datasets was determined to be the optimal size for statistical analysis and to allow for independent replicates, given the scarcity of cells isolated from each fetal sample. The sample size and experimental replicates for *in vitro* experiments are subsequently indicated in all accompanying figure legends or supplementary tables. Sample size was determined to be adequate based on the magnitude and consistency of measurable differences between groups. Investigators were not blinded, and samples were equally divided between treatments, i.e. gRNA received. Further details on dataset analysis and experimental technique are detailed in Supplementary Materials and Methods.

Magnetic isolation of $CD4^+$ T cells and fluorescence activated cell sorting (FACS) for sequencing and cell culture

Prior to FACS, fetal splenocytes and adult PBMCs were pre-enriched for $CD4^+$ T cells using the EasySep Human $CD4^+$ T cell isolation kit (#17952, STEMCELL Technologies). In order to obtain sufficient numbers of adult regulatory T (T_{reg}) cells for epigenetic analyses, adult PBMCs were also pre-enriched for $CD4^+CD127^{lo}$ T cells using the Human $CD4^+CD127^{lo}$ T cell Pre-enrichment kit (#19231, STEMCELL Technologies). Enriched cell fractions were incubated in FACS staining buffer (phosphate-buffered saline, PBS, with 2% HI-FBS and 2mM EDTA) with fluorochrome-conjugated anti-human surface monoclonal antibodies (mAbs): CD25 FITC (2A3, BD Biosciences), CD127 PE/BV421 (hIL-7R-M21, BD Pharmingen), CD45RA PE-CF594 (HI100, BD Horizon), CD4 PE-Cy7 (SK3, BD Pharmingen), CD27 eFluor780 (O323, ThermoFisher Scientific). All cells were stained with

the live-dead marker (GhostDye Violet 510; Tonbo Biosciences) to exclude dead cells. Cells were sorted into supplemented RPMI (10% HI-FBS, 300 mg/L L-glutamine, 10 U/mL penicillin, and 10 μg/mL streptomycin) based on gating in Fig. S1. All sorts were carried out on a BD FACS Aria III.

RNAseq for *ex vivo* sorted cells

RNAseq was carried out for 2.5×10^5 cells for 4 biological replicates of adult and fetal naïve and T_{reg} cells. RNA was extracted and purified with the Nucleospin RNA kit (Machery-Nagel) and assessed for quality by RNA Pico (Agilent Technologies). Library preparation and sequencing on a HiSeq300 were carried out by the Technology Center for Genomics and Bioinformatics (TCGB) core at University of California, Los Angeles.

RNAseq for adult and fetal induced T_{reg} populations

4 biological replicates of sorted adult or fetal naïve T cells were stimulated in U-bottomed 96 wells with 5 μl of Immunocult Human T cell Activator (CD3/CD28/CD2 tetramers, STEMCELL Technologies) in 200 μl of culture media (RPMI-1640 supplemented with 10% HI-FBS (heat inactivated fetal bovine serum), 300 mg/L L-glutamine, 10 U/mL penicillin, and 10 μg/mL streptomycin, 10 mM HEPES, 1X MEM-NEAA, β-mercaptoethanol). Exogenous IL-2 (10 ng/ml, Peprotech) and TGF-β (50 ng/ml, Peprotech) were added according to the relevant experimental setup. 100 μl media changes were performed every two days starting from the first day of stimulation. At day 6 post-induction, RNA from 2.5×10^4 iT_{reg} cells was extracted and purified with the Nucleospin XS RNA kit (Machery-Nagel) and assessed for quality by RNA Pico (Agilent Technologies). Ribosomal RNA was removed using the NEBNext® Poly(A) mRNA Magnetic Isolation Module (New England Biolabs), and library preparation was carried out using the NEBNext® Ultra™ II Directional RNA Library Prep Kit for Illumina® (New England Biolabs). Sequencing on a HiSeq4000 was carried out by the Center for Advanced Technology core at UCSF.

Flow cytometry staining in sorted naïve and T_{reg} cells

Sorted naïve and T_{reg} cells from fetal and adult samples were incubated in FACS buffer with fluorochome-conjugated, anti-human surface mAbs. Fixation and permeabilization was performed using the Foxp3/Transcription Factor Staining Buffer set (Tonbo Biosciences). All cells were stained with a live/dead marker (GhostDye Violet 510; Tonbo Biosciences) to exclude dead cells from analysis. All data were acquired with an LSRII flow cytometer (BD Biosciences) and analyzed with FlowJo (BD Biosciences) software. $Helios^+$ and $Helios^-$ gates were set based on the clearly positive and negative populations seen in adult T_{reg} samples; all adult naïve T cell samples were observed to be fully within the $Helios^-$ population, and were subsequently used to define the $Helios^-$ gate for subsequent experiments as a biological negative control.

T_{reg} induction assays

Sorted adult or fetal naïve T cells were differentiated into T_{reg} cells as detailed above according to the relevant experimental setup. For T_{reg} induction with TGF-β blockade, 2.5 μg/ml or 0.5 μg/ml of neutralizing anti-TGF-β (1D11, R&D Systems) antibody was added to

the culture medium where specified. Cells were cultured and harvested after 1, 3 and 5 days for analysis by flow cytometry. 100 μl media changes were performed every two days starting from the first day of stimulation. Cells were stained, fixed and permeabilized as detailed in flow cytometry staining. All data were acquired with an LSRII flow cytometer (BD Biosciences) and analyzed with FlowJo (BD Biosciences) software.

CRISPR-Cas9 editing of the Helios locus

CRISPR-Cas9 editing was carried out as previously detailed (94, 95). Cas9 gRNA ribonucleoproteins (RNPs) were assembled before experiments by assembling the gRNAs through incubating 160 μM of crRNA with 160 μM of tracrRNA (Dharmacon) at a 1:1 ratio for 30 minutes at 37°C to a final concentration of 80 μM. Assembled gRNAs are then subsequently incubated with 40 μM of Cas9-NLS (QB3 MacroLab, UC Berkeley) at a 1:1 ratio for 15 minutes at 37°C for a final concentration of 20 μM RNPs. Nucleofection was performed using the Amaxa P3 Primary Cell 96-well Nucleofector kit and 4D-Nucleofector (Lonza). 1×10^5 sorted fetal naïve T cells per well were stimulated overnight in 96-well plates pre-coated with anti-CD3 antibodies (1 μg/mL, HIT3a, BD Biosciences), and supplemented with soluble anti-CD28 antibodies (2 μg/mL, CD28.2, BD Biosciences) and IL-2 (10 ng/ml, Peprotech). Stimulated fetal naïve T cells were washed with PBS, and resuspended in 20 μl of P3 solution. 5 μl of the final 20 μM RNP solution was added, along with 1 μl of 100 μM HDRT solution. Cells were gently mixed, and transferred to the 96-well shuttle device. Cells were electroporated using program EH-115 on the Amaxa 4D-Nucleofector (Lonza). 80 μl of prewarmed culture media was added immediately post-nucleofection, and cells were allowed to recover for 15 minutes at 37°C. Nucleofected cells were then transferred into a 96-well U-bottom plate, and additional culture media added to a final volume of 200 μl. After 5 hours, cells were spun down and 150 μl of the culture media changed to increase cell viability and left to incubate overnight. Cells were stimulated the next day for T_{reg} induction assays as detailed above, and harvested at Day 6 for analysis.

RNAseq for Helios^{KO} and Helios^{WT} T_{reg} populations

CRISPR-Cas9 mediated Helios knockout in 6 biological replicates of fetal naïve T cells was performed as described above using Helios gRNA1 or the NT control guide for (all samples paired across nucleofection conditions). Cells were stimulated for T_{reg} induction assays as detailed above, and 2.5×10^4 iT_{reg} cells harvested at Day 6 for RNA extraction and analysis. RNA extraction, library preparation and sequencing were carried out as for fetal and adult iT_{reg} populations.

Cytokine bead assays

100ul of culture supernatant were collected at D3 and D5 of T_{reg} differentiation with IL-2 only or in the presence of added TGF-β. Supernatants collected at D5 of T_{reg} differentiation after CRISPR-Cas9 mediated Helios knockout were also analyzed. Supernatants were harvested and stored at −80°C prior to analysis. IL-10 (#558274) and IFN-γ (#558269) concentrations were measured using the Cytokine Bead Assay (CBA) Flex kits (BD Biosciences).

Statistical analyses

All statistical analyses were performed using R (cran.r-project.org, v3.5.2) and Bioconductor (www.bioconductor.org). Tests were specified with each experiment in each figure legend, and $p<0.05$ level of confidence was accepted for statistical significance. All statistical tests are non-parametric and two-sided unless mentioned. Paired testing was used when comparisons were made within the same sample in order to increase resistance towards outlier effects, and are specified in the figure legends. Kruskal-Wallis test and Dunn's post-test with Bonferroni correction were performed using the PMCMRplus (v1.4.1) package. Graphs were made using the ggplot2 (v3.1.0), ggrepel (v0.8.0) and cowplot (v0.9.4) R packages. Heatmaps were generated with the ComplexHeatmap (v1.12.0) R package.

Supplementary Material

Refer to Web version on PubMed Central for supplementary material.

Acknowledgements:

We would like to thank S. Fisher, P. Odorizzi, E. Rackaityte, J. Halkias, D. Bunis, J. Mold, J.M, McCune, and J.Y. Lim for helpful discussion. We thank D. Simeonov and K. Schumann for help with CRISPR-Cas9 editing. We thank M. Nguyen for advice and help with cell fixation and DNA extraction for TSDR analysis. We thank R. Krishnakumar, A. Chen, S. Thomas and R. Thomas for their technical help with ChIPseq and advice on bioinformatics analyses. Bioinformatics analyses for genome mapping and bigwig file generation for ATACseq was carried out by the Gladstone Bioinformatics Core at the Gladstone Institutes. Bioinformatic analyses for RNAseq in *ex vivo* naïve and T_{reg} cells were carried out by the Technology Center for Genomics and Bioinformatics (TCGB) at University of California, Los Angeles. Sequencing for ChIPseq and RNAseq in iT_{reg} cells were carried out at the Center for Advanced Technologies (CAT) Core at UCSF.

Funding: This work was supported by an Agency for Science, Technology and Research (A*STAR, Singapore) National Science Scholarship (PhD) awarded to M.N, and research grants NIH K08HD067295 and R21AI120032 to T.D.B., who was also supported by an award from the Preterm Birth Initiative of the Burroughs Wellcome Fund. T.L.R. was supported by the UCSF Medical Scientist Training Program (T32GM007618) and the UCSF Endocrinology Training Grant (T32DK007418). A.M. holds a Career Award for Medical Scientists from the Burroughs Wellcome Fund, has received funding from the Innovative Genomics Insitute (IGI) and the Parker Institute for Cancer Immunotherapy (PICI), and is an investigator at the Chan Zuckerberg Biohub. We also thank the Flow Cytometry Core at UCSF, supported by the Diabetes Research Center grant NIH P30 DK063720, and Shared Instrument Grant 1S10OD021822–01.

References

1. Mucida D, Kutchukhidze N, Erazo A, Russo M, Lafaille JJ, de Lafaille M. A. Curotto, Oral tolerance in the absence of naturally occurring Tregs, J. Clin. Invest. 115, 1923–1933 (2005). [PubMed: 15937545]
2. Coombes JL, Siddiqui KRR, Arancibia-Cárcamo CV, Hall J, Sun CM, Belkaid Y, Powrie F, A functionally specialized population of mucosal CD103+ DCs induces Foxp3+ regulatory T cells via a TGF-beta and retinoic acid-dependent mechanism, J. Exp. Med. 204, 1757–1764 (2007). [PubMed: 17620361]
3. Haribhai D, Williams JB, Jia S, Nickerson D, Schmitt EG, Edwards B, Ziegelbauer J, Yassai M, Li S-H, Relland LM, Wise PM, Chen A, Zheng Y-Q, Simpson PM, Gorski J, Salzman NH, Hessner MJ, Chatila TA, Williams CB, A requisite role for induced regulatory T cells in tolerance based on expanding antigen receptor diversity, Immunity 35, 109–122 (2011). [PubMed: 21723159]
4. Zhu J, Paul WE, CD4 T cells: fates, functions, and faults, Blood 112, 1557–1569 (2008). [PubMed: 18725574]
5. Zhu J, Yamane H, Paul WE, Differentiation of effector CD4 T cell populations (*), Annu. Rev. Immunol. 28, 445–489 (2010). [PubMed: 20192806]

6. Sundrud MS, Nolan MA, Synergistic and combinatorial control of T cell activation and differentiation by transcription factors, Curr. Opin. Immunol. 22, 286–292 (2010). [PubMed: 20399089]
7. Chen W, Jin W, Hardegen N, Lei K-J, Li L, Marinos N, McGrady G, Wahl SM, Conversion of peripheral CD4+CD25- naive T cells to CD4+CD25+ regulatory T cells by TGF-beta induction of transcription factor Foxp3, J. Exp. Med. 198, 1875–1886 (2003). [PubMed: 14676299]
8. Fantini MC, Becker C, Monteleone G, Pallone F, Galle PR, Neurath MF, Cutting edge: TGF-beta induces a regulatory phenotype in CD4+CD25- T cells through Foxp3 induction and down-regulation of Smad7, J. Immunol. 172, 5149–5153 (2004). [PubMed: 15100250]
9. Chen Y, Kim JK, Hirning AJ, Josi K, Bennett MR, Emergent genetic oscillations in a synthetic microbial consortium, Science 349, 986–989 (2015). [PubMed: 26315440]
10. Brunkow ME, Jeffery EW, Hjerrild KA, Paeper B, Clark LB, Yasayko SA, Wilkinson JE, Galas D, Ziegler SF, Ramsdell F, Disruption of a new forkhead/winged-helix protein, scurfin, results in the fatal lymphoproliferative disorder of the scurfy mouse, Nat. Genet. 27, 68–73 (2001). [PubMed: 11138001]
11. Wildin RS, Ramsdell F, Peake J, Faravelli F, Casanova JL, Buist N, Levy-Lahad E, Mazzella M, Goulet O, Perroni L, Bricarelli FD, Byrne G, McEuen M, Proll S, Appleby M, Brunkow ME, X-linked neonatal diabetes mellitus, enteropathy and endocrinopathy syndrome is the human equivalent of mouse scurfy, Nat. Genet. 27, 18–20 (2001). [PubMed: 11137992]
12. Bennett CL, Christie J, Ramsdell F, Brunkow ME, Ferguson PJ, Whitesell L, Kelly TE, Saulsbury FT, Chance PF, Ochs HD, The immune dysregulation, polyendocrinopathy, enteropathy, X-linked syndrome (IPEX) is caused by mutations of FOXP3, Nat. Genet. 27, 20–21 (2001). [PubMed: 11137993]
13. Khattri R, Cox T, Yasayko S-A, Ramsdell F, An essential role for Scurfin in CD4+CD25+ T regulatory cells, Nat Immunol 4, 337–342 (2003). [PubMed: 12612581]
14. Fontenot JD, Gavin MA, Rudensky AY, Foxp3 programs the development and function of CD4+CD25+ regulatory T cells, Nat Immunol 4, 330–336 (2003). [PubMed: 12612578]
15. Sakaguchi S, Naturally arising Foxp3-expressing CD25+ CD4+ regulatory T cells in immunological tolerance to self and non-self, Nat Immunol (2005).
16. Xavier-da-Silva MM, Moreira-Filho CA, Suzuki E, Patricio F, Coutinho A, Carneiro-Sampaio M, Fetal-onset IPEX: report of two families and review of literature, Clin. Immunol. 156, 131–140 (2015). [PubMed: 25546394]
17. Vasiljevic A, Poreau B, Bouvier R, Lachaux A, Arnoult C, Fauré J, Cordier MP, Ray PF, Immune dysregulation, polyendocrinopathy, enteropathy, X-linked syndrome and recurrent intrauterine fetal death, Lancet 385, 2120 (2015). [PubMed: 26009232]
18. Rae W, Gao Y, Bunyan D, Holden S, Gilmour K, Patel S, Wellesley D, Williams A, A novel FOXP3 mutation causing fetal akinesia and recurrent male miscarriages, Clin. Immunol. 161, 284–285 (2015). [PubMed: 26387632]
19. Reichert SL, McKay EM, Moldenhauer JS, Identification of a novel nonsense mutation in the FOXP3 gene in a fetus with hydrops--Expanding the phenotype of IPEX syndrome, Am. J. Med. Genet. A 170A, 226–232 (2016). [PubMed: 26395338]
20. Shehab O, Tester DJ, Ackerman NC, Cowchock FS, Ackerman MJ, Whole genome sequencing identifies etiology of recurrent male intrauterine fetal death, Prenat. Diagn. 37, 1040–1045 (2017). [PubMed: 28833278]
21. Burt TD, Fetal Regulatory T Cells and Peripheral Immune Tolerance In Utero: Implications for Development and Disease, Am J Reprod Immunol 69, 346–358 (2013). [PubMed: 23432802]
22. Bacchetta R, Barzaghi F, Roncarolo MG, Rose NR, Ed. From IPEX syndrome to FOXP3 mutation: a lesson on immune dysregulation, Annals of the New York Academy of Sciences 1417, 5–22 (2018). [PubMed: 26918796]
23. Michaelsson J, Mold JE, McCune JM, Nixon DF, Regulation of T Cell Responses in the Developing Human Fetus, J. Immunol. 176, 5741–5748 (2006). [PubMed: 16670279]
24. Mold JE, Michaelsson J, Burt TD, Muench MO, Beckerman KP, Busch MP, Lee TH, Nixon DF, McCune JM, Maternal Alloantigens Promote the Development of Tolerogenic Fetal Regulatory T Cells in Utero, Science 322, 1562–1565 (2008). [PubMed: 19056990]

25. Mold JE, Venkatasubrahmanyam S, Burt TD, Michaelsson J, Rivera JM, Galkina SA, Weinberg K, Stoddart CA, McCune JM, Fetal and Adult Hematopoietic Stem Cells Give Rise to Distinct T Cell Lineages in Humans, Science 330, 1695–1699 (2010). [PubMed: 21164017]
26. Bronevetsky Y, Burt TD, McCune JM, Lin28b Regulates Fetal Regulatory T Cell Differentiation through Modulation of TGF-β Signaling, The Journal of Immunology 197, 4344–4350 (2016). [PubMed: 27793996]
27. Tripathi SK, Lahesmaa R, Transcriptional and epigenetic regulation of T-helper lineage specification, Immunological Reviews 261, 62–83 (2014). [PubMed: 25123277]
28. Nguyen MLT, Jones SA, Prier JE, Russ BE, Transcriptional Enhancers in the Regulation of T Cell Differentiation, Front Immunol 6, 462 (2015). [PubMed: 26441967]
29. Ohkura N, Hamaguchi M, Morikawa H, Sugimura K, Tanaka A, Ito Y, Osaki M, Tanaka Y, Yamashita R, Nakano N, Huehn J, Fehling HJ, Sparwasser T, Nakai K, Sakaguchi S, T Cell Receptor Stimulation-Induced Epigenetic Changes and Foxp3 Expression Are Independent and Complementary Events Required for Treg Cell Development, Immunity 37, 785–799 (2012). [PubMed: 23123060]
30. Kitagawa Y, Ohkura N, Kidani Y, Vandenbon A, Hirota K, Kawakami R, Yasuda K, Motooka D, Nakamura S, Kondo M, Taniuchi I, Kohwi-Shigematsu T, Sakaguchi S, Guidance of regulatory T cell development by Satb1-dependent super-enhancer establishment, Nat Immunol 18, 173–183 (2017). [PubMed: 27992401]
31. Zheng Y, Josefowicz S, Chaudhry A, Peng XP, Forbush K, Rudensky AY, Role of conserved non-coding DNA elements in the Foxp3 gene in regulatory T-cell fate, Nature 463, 808–812 (2010). [PubMed: 20072126]
32. Arvey A, van der Veeken J, Plitas G, Rich SS, Concannon P, Rudensky AY, Genetic and epigenetic variation in the lineage specification of regulatory T cells, Elife 4, e07571 (2015).
33. Hill JA, Feuerer M, Tash K, Haxhinasto S, Perez J, Melamed R, Mathis D, Benoist C, Foxp3 Transcription-Factor-Dependent and -Independent Regulation of the Regulatory T Cell Transcriptional Signature, Immunity 27, 786–800 (2007). [PubMed: 18024188]
34. Fu W, Ergun A, Lu T, Hill JA, Haxhinasto S, Fassett MS, Gazit R, Adoro S, Glimcher L, Chan S, Kastner P, Rossi D, Collins JJ, Mathis D, Benoist C, A multiply redundant genetic switch "locks in" the transcriptional signature of regulatory T cells, Nat Immunol 13, 972–980 (2012). [PubMed: 22961053]
35. Curiel TJ, Coukos G, Zou L, Alvarez X, Cheng P, Mottram P, Evdemon-Hogan M, Conejo-Garcia JR, Zhang L, Burow M, Zhu Y, Wei S, Kryczek I, Daniel B, Gordon A, Myers L, Lackner A, Disis ML, Knutson KL, Chen L, Zou W, Specific recruitment of regulatory T cells in ovarian carcinoma fosters immune privilege and predicts reduced survival, Nature Medicine 10, 942–949 (2004).
36. Miyara M, Sakaguchi S, Natural regulatory T cells: mechanisms of suppression, Trends Mol Med 13, 108–116 (2007). [PubMed: 17257897]
37. Cao Z, Wara AK, Icli B, Sun X, Packard RRS, Esen F, Stapleton CJ, Subramaniam M, Kretschmer K, Apostolou I, von Boehmer H, Hansson GK, Spelsberg TC, Libby P, Feinberg MW, Kruppel-like Factor KLF10 Targets Transforming Growth Factor- 1 to Regulate CD4+CD25- T Cells and T Regulatory Cells, Journal of Biological Chemistry 284, 24914–24924 (2009). [PubMed: 19602726]
38. Xiong Y, Khanna S, Grzenda AL, Sarmento OF, Svingen PA, Lomberk GA, Urrutia RA, Faubion WA, Polycomb Antagonizes p300/CREB-binding Protein-associated Factor to Silence FOXP3 in a Kruppel-like Factor-dependent Manner, Journal of Biological Chemistry 287, 34372–34385 (2012). [PubMed: 22896699]
39. Xiong Y, Svingen PA, Sarmento OO, Smyrk TC, Dave M, Khanna S, Lomberk GA, Urrutia RA, Faubion WA, Differential coupling of KLF10 to Sin3-HDAC and PCAF regulates the inducibility of the FOXP3 gene, AJP: Regulatory, Integrative and Comparative Physiology 307, R608–R620 (2014).
40. Thornton AM, Korty PE, Tran DQ, Wohlfert EA, Murray PE, Belkaid Y, Shevach EM, Expression of Helios, an Ikaros Transcription Factor Family Member, Differentiates Thymic-Derived from Peripherally Induced Foxp3+ T Regulatory Cells, The Journal of Immunology 184, 3433–3441 (2010). [PubMed: 20181882]

41. Kim H-J, Barnitz RA, Kreslavsky T, Brown FD, Moffett H, Lemieux ME, Kaygusuz Y, Meissner T, Holderried TAW, Chan S, Kastner P, Haining WN, Cantor H, Stable inhibitory activity of regulatory T cells requires the transcription factor Helios, Science 350, 334–339 (2015). [PubMed: 26472910]
42. Sebastian M, Lopez-Ocasio M, Metidji A, Rieder SA, Shevach EM, Thornton AM, Helios Controls a Limited Subset of Regulatory T Cell Functions, The Journal of Immunology 196, 144–155 (2016). [PubMed: 26582951]
43. Pan F, Yu H, Dang EV, Barbi J, Pan X, Grosso JF, Jinasena D, Sharma SM, McCadden EM, Getnet D, Drake CG, Liu JO, Ostrowski MC, Pardoll DM, Eos mediates Foxp3-dependent gene silencing in CD4+ regulatory T cells, Science 325, 1142–1146 (2009). [PubMed: 19696312]
44. Morikawa H, Ohkura N, Vandenbon A, Itoh M, Nagao-Sato S, Kawaji H, Lassmann T, Carninci P, Hayashizaki Y, Forrest ARR, Standley DM, Date H, Sakaguchi S, FANTOM Consortium, Itoh M, Sakaguchi S, Differential roles of epigenetic changes and Foxp3 expression in regulatory T cell-specific transcriptional regulation, Proc. Natl. Acad. Sci. U.S.A. 111, 5289–5294 (2014). [PubMed: 24706905]
45. Yu A, Zhu L, Altman NH, Malek TR, A low interleukin-2 receptor signaling threshold supports the development and homeostasis of T regulatory cells, Immunity 30, 204–217 (2009). [PubMed: 19185518]
46. Joller N, Lozano E, Burkett PR, Patel B, Xiao S, Zhu C, Xia J, Tan TG, Sefik E, Yajnik V, Sharpe AH, Quintana FJ, Mathis D, Benoist C, Hafler DA, Kuchroo VK, Treg cells expressing the coinhibitory molecule TIGIT selectively inhibit proinflammatory Th1 and Th17 cell responses, Immunity 40, 569–581 (2014). [PubMed: 24745333]
47. Furlan SN, Watkins B, Tkachev V, Cooley S, Panoskaltsis-Mortari A, Betz K, Brown M, Hunt DJ, Schell JB, Zeleski K, Yu A, Giver CR, Waller EK, Miller JS, Blazar BR, Kean LS, Systems analysis uncovers inflammatory Th/Tc17-driven modules during acute GVHD in monkey and human T cells, Blood 128, 2568–2579 (2016). [PubMed: 27758873]
48. Takimoto T, Wakabayashi Y, Sekiya T, Inoue N, Morita R, Ichiyama K, Takahashi R, Asakawa M, Muto G, Mori T, Hasegawa E, Saika S, Shizuya S, Hara T, Nomura M, Yoshimura A, Smad2 and Smad3 are redundantly essential for the TGF-beta-mediated regulation of regulatory T plasticity and Th1 development, The Journal of Immunology 185, 842–855 (2010). [PubMed: 20548029]
49. Delgoffe GM, Woo S-R, Turnis ME, Gravano DM, Guy C, Overacre AE, Bettini ML, Vogel P, Finkelstein D, Bonnevier J, Workman CJ, Vignali DAA, Stability and function of regulatory T cells is maintained by a neuropilin-1-semaphorin-4a axis, Nature 501, 252–256 (2013). [PubMed: 23913274]
50. Travis MA, Sheppard D, TGF-β activation and function in immunity, Annu. Rev. Immunol. 32, 51–82 (2014). [PubMed: 24313777]
51. Ocklenburg F, Moharregh-Khiabani D, Geffers R, Janke V, Pfoertner S, Garritsen H, Groebe L, Klempnauer J, Dittmar KEJ, Weiss S, Buer J, Probst-Kepper M, UBD, a downstream element of FOXP3, allows the identification of LGALS3, a new marker of human regulatory T cells, Lab. Invest. 86, 724–737 (2006). [PubMed: 16702978]
52. Probst-Kepper M, Geffers R, Kröger A, Viegas N, Erck C, Hecht H-J, Lünsdorf H, Roubin R, Moharregh-Khiabani D, Wagner K, Ocklenburg F, Jeron A, Garritsen H, Arstila TP, Kekäläinen E, Balling R, Hauser H, Buer J, Weiss S, GARP: a key receptor controlling FOXP3 in human regulatory T cells, J. Cell. Mol. Med. 13, 3343–3357 (2009). [PubMed: 19453521]
53. Pesenacker AM, Wang AY, Singh A, Gillies J, Kim Y, Piccirillo CA, Nguyen D, Haining WN, Tebbutt SJ, Panagiotopoulos C, Levings MK, A Regulatory T-Cell Gene Signature Is a Specific and Sensitive Biomarker to Identify Children With New-Onset Type 1 Diabetes, Diabetes 65, 1031–1039 (2016). [PubMed: 26786322]
54. Tran DQ, Ramsey H, Shevach EM, Induction of FOXP3 expression in naive human CD4+FOXP3 T cells by T-cell receptor stimulation is transforming growth factor-beta dependent but does not confer a regulatory phenotype, Blood 110, 2983–2990 (2007). [PubMed: 17644734]
55. Edwards JP, Thornton AM, Shevach EM, Release of active TGF-β1 from the latent TGF-β1/GARP complex on T regulatory cells is mediated by integrin β8, The Journal of Immunology 193, 2843–2849 (2014). [PubMed: 25127859]

56. Wang R, Kozhaya L, Mercer F, Khaitan A, Fujii H, Unutmaz D, Expression of GARP selectively identifies activated human FOXP3+ regulatory T cells, Proc. Natl. Acad. Sci. U.S.A. 106, 13439–13444 (2009). [PubMed: 19666573]
57. Whyte WA, Orlando DA, Hnisz D, Abraham BJ, Lin CY, Kagey MH, Rahl PB, Lee TI, Young RA, Master Transcription Factors and Mediator Establish Super-Enhancers at Key Cell Identity Genes, Cell 153, 307–319 (2013). [PubMed: 23582322]
58. Lovén J, Hoke HA, Lin CY, Lau A, Orlando DA, Vakoc CR, Bradner JE, Lee TI, Young RA, Selective inhibition of tumor oncogenes by disruption of super-enhancers, Cell 153, 320–334 (2013). [PubMed: 23582323]
59. Shlyueva D, Stampfel G, Stark A, Transcriptional enhancers: from properties to genome-wide predictions, Nature Publishing Group 15, 272–286 (2014).
60. Samstein RM, Arvey A, Josefowicz SZ, Peng X, Reynolds A, Sandstrom R, Neph S, Sabo P, Kim JM, Liao W, Li MO, Leslie C, Stamatoyannopoulos JA, Rudensky AY, Foxp3 Exploits a Pre-Existent Enhancer Landscape for Regulatory T Cell Lineage Specification, Cell 151, 153–166 (2012). [PubMed: 23021222]
61. Schmidl C, Hansmann L, Lassmann T, Balwierz PJ, Kawaji H, Itoh M, Kawai J, Nagao-Sato S, Suzuki H, Andreesen R, Hayashizaki Y, Forrest ARR, Carninci P, Hoffmann P, Edinger M, Rehli M, FANTOM Consortium, The enhancer and promoter landscape of human regulatory and conventional T-cell subpopulations, Blood 123, e68–78 (2014). [PubMed: 24671953]
62. Adam RC, Yang H, Rockowitz S, Larsen SB, Nikolova M, Oristian DS, Polak L, Kadaja M, Asare A, Zheng D, Fuchs E, Pioneer factors govern super-enhancer dynamics in stem cell plasticity and lineage choice, Nature 521, 366–370 (2015). [PubMed: 25799994]
63. Wakabayashi Y, Watanabe H, Inoue J, Takeda N, Sakata J, Mishima Y, Hitomi J, Yamamoto T, Utsuyama M, Niwa O, Aizawa S, Kominami R, Bcl11b is required for differentiation and survival of alphabeta T lymphocytes, Nat Immunol 4, 533–539 (2003). [PubMed: 12717433]
64. Muthusamy N, Barton K, Leiden JM, Defective activation and survival of T cells lacking the Ets-1 transcription factor, Nature 377, 639–642 (1995). [PubMed: 7566177]
65. Sugimoto N, Oida T, Hirota K, Nakamura K, Nomura T, Uchiyama T, Sakaguchi S, Foxp3-dependent and -independent molecules specific for CD25+CD4+ natural regulatory T cells revealed by DNA microarray analysis, International Immunology 18, 1197–1209 (2006). [PubMed: 16772372]
66. Gottschalk RA, Corse E, Allison JP, Expression of Helios in peripherally induced Foxp3+ regulatory T cells, The Journal of Immunology 188, 976–980 (2012). [PubMed: 22198953]
67. Getnet D, Grosso JF, Goldberg MV, Harris TJ, Yen H-R, Bruno TC, Durham NM, Hipkiss EL, Pyle KJ, Wada S, Pan F, Pardoll DM, Drake CG, A role for the transcription factor Helios in human CD4(+)CD25(+) regulatory T cells, Molecular Immunology 47, 1595–1600 (2010). [PubMed: 20226531]
68. Paiva RS, Lino AC, Bergman M-L, Caramalho I, Sousa AE, Zelenay S, Demengeot J, Recent thymic emigrants are the preferential precursors of regulatory T cells differentiated in the periphery, Proc. Natl. Acad. Sci. U.S.A. 110, 6494–6499 (2013). [PubMed: 23576744]
69. Kimmig S, Przybylski GK, Schmidt CA, Laurisch K, Möwes B, Radbruch A, Thiel A, Two subsets of naive T helper cells with distinct T cell receptor excision circle content in human adult peripheral blood, J. Exp. Med. 195, 789–794 (2002). [PubMed: 11901204]
70. Akimova T, Beier UH, Wang L, Levine MH, Hancock WW, Molina-Paris C, Ed. Helios expression is a marker of T cell activation and proliferation, PLoS ONE 6, e24226 (2011).
71. Floess S, Freyer J, Siewert C, Baron U, Olek S, Polansky J, Schlawe K, Chang H-D, Bopp T, Schmitt E, Klein-Hessling S, Serfling E, Hamann A, Huehn J, Marrack P, Ed. Epigenetic control of the foxp3 locus in regulatory T cells, PLoS Biol. 5, e38 (2007).
72. Koenecke C, Czeloth N, Bubke A, Schmitz S, Kissenpfennig A, Malissen B, Huehn J, Ganser A, Förster R, Prinz I, Alloantigen-specific de novo-induced Foxp3+ Treg revert in vivo and do not protect from experimental GVHD, Eur. J. Immunol. 39, 3091–3096 (2009). [PubMed: 19750478]
73. Beres A, Komorowski R, Mihara M, Drobyski WR, Instability of Foxp3 Expression Limits the Ability of Induced Regulatory T Cells to Mitigate Graft versus Host Disease, Clinical Cancer Research 17, 3969–3983 (2011). [PubMed: 21558402]

74. Jonuleit H, Schmitt E, Stassen M, Tuettenberg A, Knop J, Enk AH, Identification and functional characterization of human CD4(+)CD25(+) T cells with regulatory properties isolated from peripheral blood, J. Exp. Med. 193, 1285–1294 (2001). [PubMed: 11390435]
75. Baine I, Basu S, Ames R, Sellers RS, Macian F, Helios Induces Epigenetic Silencing of Il2 Gene Expression in Regulatory T Cells, J. Immunol. 190, 1008–1016 (2013). [PubMed: 23275607]
76. Gasteiger G, Kastenmuller W, Foxp3+ Regulatory T-cells and IL-2: The Moirai of T-cell Fates? Front Immunol 3, 179 (2012). [PubMed: 22807926]
77. Takatori H, Kawashima H, Matsuki A, Meguro K, Tanaka S, Iwamoto T, Sanayama Y, Nishikawa N, Tamachi T, Ikeda K, Suto A, Suzuki K, Kagami S-I, Hirose K, Kubo M, Hori S, Nakajima H, Helios Enhances Treg Cell Function in Cooperation With FoxP3, Arthritis Rheumatol 67, 1491–1502 (2015). [PubMed: 25733061]
78. Fu S-H, Yeh L-T, Chu C-C, Yen BL-J, Sytwu H-K, New insights into Blimp-1 in T lymphocytes: a divergent regulator of cell destiny and effector function, J. Biomed. Sci. 24, 49 (2017). [PubMed: 28732506]
79. Onodera A, Kokubo K, Nakayama T, Epigenetic and Transcriptional Regulation in the Induction, Maintenance, Heterogeneity, and Recall-Response of Effector and Memory Th2 Cells, Front Immunol 9, 2929 (2018). [PubMed: 30619290]
80. Quirion MR, Gregory GD, Umetsu SE, Winandy S, Brown MA, Cutting edge: Ikaros is a regulator of Th2 cell differentiation, The Journal of Immunology 182, 741–745 (2009). [PubMed: 19124715]
81. Wong LY, Hatfield JK, Brown MA, Ikaros sets the potential for Th17 lineage gene expression through effects on chromatin state in early T cell development, J. Biol. Chem. 288, 35170–35179 (2013). [PubMed: 24145030]
82. Wheaton JD, Yeh C-H, Ciofani M, Cutting Edge: c-Maf Is Required for Regulatory T Cells To Adopt RORγt+ and Follicular Phenotypes, The Journal of Immunology 199, 3931–3936 (2017). [PubMed: 29127150]
83. Choi J-M, Bothwell ALM, The nuclear receptor PPARs as important regulators of T-cell functions and autoimmune diseases, Mol. Cells 33, 217–222 (2012). [PubMed: 22382683]
84. Kaminuma O, Kitamura N, Nishito Y, Nemoto S, Tatsumi H, Mori A, Hiroi T, Downregulation of NFAT3 Due to Lack of T-Box Transcription Factor TBX5 Is Crucial for Cytokine Expression in T Cells, The Journal of Immunology 200, 92–100 (2018). [PubMed: 29180489]
85. Li Q, Zou J, Wang M, Ding X, Chepelev I, Zhou X, Zhao W, Wei G, Cui J, Zhao K, Wang HY, Wang R-F, Critical role of histone demethylase Jmjd3 in the regulation of CD4+ T-cell differentiation, Nat Commun 5, 5780 (2014). [PubMed: 25531312]
86. Shevach EM, Mechanisms of foxp3+ T regulatory cell-mediated suppression, Immunity 30, 636–645 (2009). [PubMed: 19464986]
87. Sridharan R, Smale ST, Predominant interaction of both Ikaros and Helios with the NuRD complex in immature thymocytes, Journal of Biological Chemistry 282, 30227–30238 (2007). [PubMed: 17681952]
88. Zhao S, Liu W, Li Y, Liu P, Li S, Dou D, Wang Y, Yang R, Xiang R, Liu F, Song C, Ed. Alternative Splice Variants Modulates Dominant-Negative Function of Helios in T-Cell Leukemia, PLoS ONE 11, e0163328 (2016).
89. Cai Q, Dierich A, Oulad-Abdelghani M, Chan S, Kastner P, Helios deficiency has minimal impact on T cell development and function, The Journal of Immunology 183, 2303–2311 (2009). [PubMed: 19620299]
90. Yang S, Fujikado N, Kolodin D, Benoist C, Mathis D, Regulatory T cells generated early in life play a distinct role in maintaining self-tolerance, Science, 1–9 (2015).
91. Smith H, Chen IM, Kubo R, Tung KS, Neonatal thymectomy results in a repertoire enriched in T cells deleted in adult thymus, Science 245, 749–752 (1989). [PubMed: 2788921]
92. Kim YC, Bhairavabhotla R, Yoon J, Golding A, Thornton AM, Tran DQ, Shevach EM, Oligodeoxynucleotides stabilize Helios-expressing Foxp3+ human T regulatory cells during in vitro expansion, Blood 119, 2810–2818 (2012). [PubMed: 22294730]

93. Thornton AM, Lu J, Korty PE, Kim YC, Martens C, Sun PD, Shevach EM, Helios+ and Helios- Treg subpopulations are phenotypically and functionally distinct and express dissimilar TCR repertoires, Eur. J. Immunol. 112, 137 (2019).

94. Schumann K, Lin S, Boyer E, Simeonov DR, Subramaniam M, Gate RE, Haliburton GE, Ye CJ, Bluestone JA, Doudna JA, Marson A, Generation of knock-in primary human T cells using Cas9 ribonucleoproteins, Proc. Natl. Acad. Sci. U.S.A. 112, 10437–10442 (2015). [PubMed: 26216948]

95. Hultquist JF, Schumann K, Woo JM, Manganaro L, McGregor MJ, Doudna J, Simon V, Krogan NJ, Marson A, A Cas9 Ribonucleoprotein Platform for Functional Genetic Studies of HIV-Host Interactions in Primary Human T Cells, Cell Rep 17, 1438–1452 (2016). [PubMed: 27783955]

96. Robinson MD, McCarthy DJ, Smyth GK, edgeR: a Bioconductor package for differential expression analysis of digital gene expression data, Bioinformatics 26, 139–140 (2010). [PubMed: 19910308]

97. McCarthy DJ, Chen Y, Smyth GK, Differential expression analysis of multifactor RNA-Seq experiments with respect to biological variation, Nucleic Acids Research 40, 4288–4297 (2012). [PubMed: 22287627]

98. Liberzon A, Birger C, Thorvaldsdóttir H, Ghandi M, Mesirov JP, Tamayo P. The Molecular Signatures Database (MSigDB) hallmark gene set collection. Cell Syst. 1:417–425 (2015). [PubMed: 26771021]

99. Buenrostro JD, Giresi PG, Zaba LC, Chang HY, Greenleaf WJ, Transposition of native chromatin for fast and sensitive epigenomic profiling of open chromatin, DNA-binding proteins and nucleosome position, Nat Meth 10, 1213–1218 (2013).

100. Buenrostro JD, Wu B, Chang HY, Greenleaf WJ, ATAC-seq: A Method for Assaying Chromatin Accessibility Genome-Wide, Curr Protoc Mol Biol 109, 21.29.1–9 (2015).

101. Collas P, A chromatin immunoprecipitation protocol for small cell numbers, Methods Mol. Biol. 791, 179–193 (2011). [PubMed: 21913080]

102. Love MI, Huber W, Anders S, Moderated estimation of fold change and dispersion for RNA-seq data with DESeq2, Genome Biol. 15, 550 (2014). [PubMed: 25516281]

103. Heinz S, Benner C, Spann N, Bertolino E, Lin YC, Laslo P, Cheng JX, Murre C, Singh H, Glass CK, Simple Combinations of Lineage-Determining Transcription Factors Prime cis-Regulatory Elements Required for Macrophage and B Cell Identities, Molecular Cell 38, 576–589 (2010). [PubMed: 20513432]

104. Labun K, Montague TG, Gagnon JA, Thyme SB, Valen E, CHOPCHOP v2: a web tool for the next generation of CRISPR genome engineering, Nucleic Acids Research 44, W272–6 (2016). [PubMed: 27185894]

105. Richardson CD, Ray GJ, Bray NL, Corn JE, Non-homologous DNA increases gene disruption efficiency by altering DNA repair outcomes, Nat Commun 7, 12463 (2016). [PubMed: 27530320]

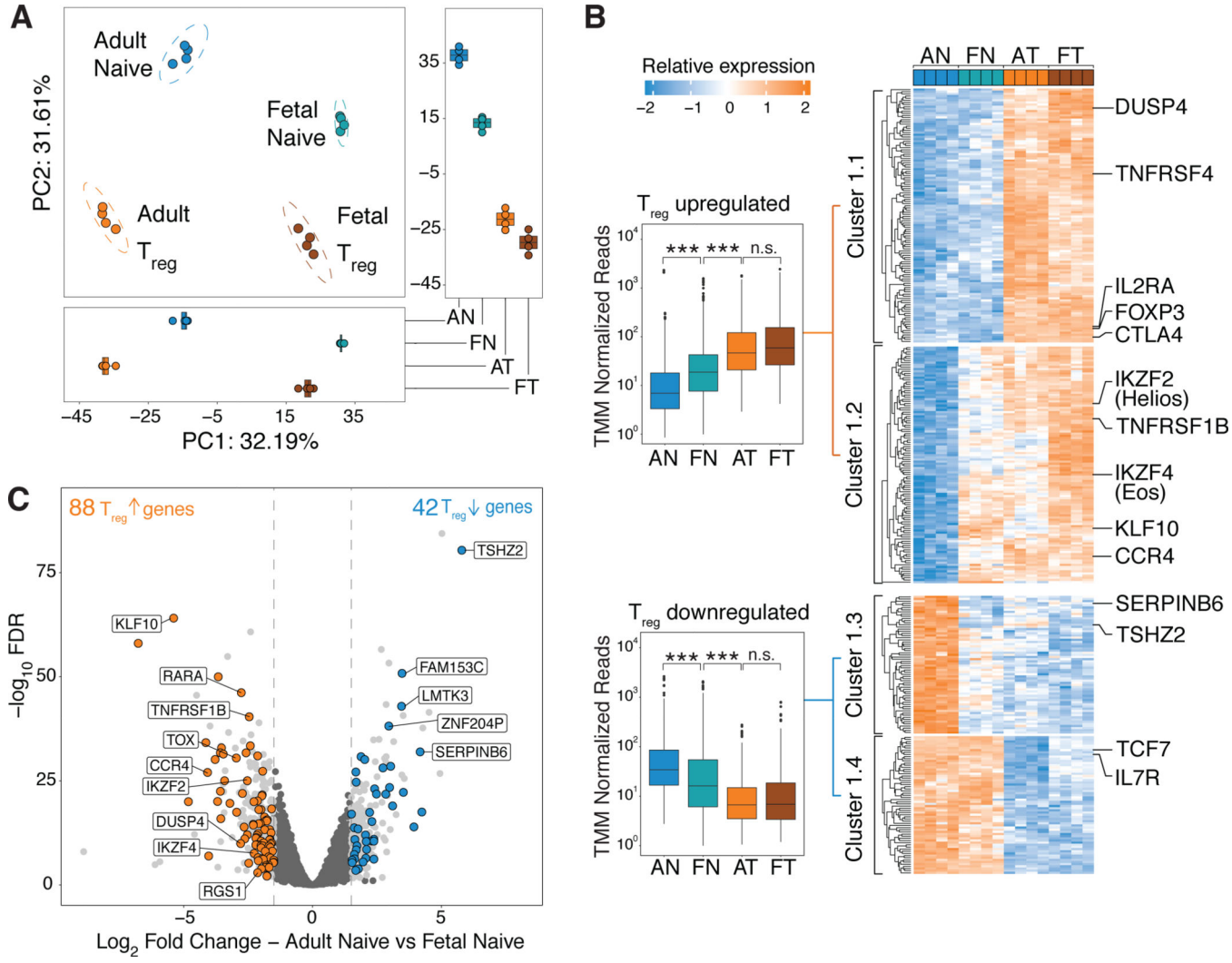

Figure 1. Fetal naïve T cells have expression of a partial T_{reg} transcriptome.

(A) Principal Component Analysis (PCA) plot of RNAseq data comparing adult naïve (AN), fetal naïve (FN), adult T_{reg} (AT) and fetal T_{reg} (FT) cells. Boxplots show scores for PC1 (bottom) and PC2 (right).

(B) Heatmap shows relative expression levels of T_{reg}-specific differentially expressed (DE) genes in AN, FN, AT and FT cells. Clusters are labeled and defined by k-means clustering. Genes associated with T_{reg} and naïve T cell function are labeled. Boxplots (left) show the averaged trimmed mean of M values (TMM) normalized reads across all upregulated (top, Cluster 1&2) and downregulated (bottom, Cluster 3&4) genes. Kruskal-Wallis test and Dunn's multiple comparison test with Bonferroni correction for multiple testing, *** $p<0.001$, n.s., $p>0.05$ (n = 4 biological replicates per group).

(C) Volcano plot of DE (log_2 fold change >1.5, p.adj<0.05) genes in fetal and adult naïve T cells, all DE genes in light grey. Dotted lines (grey) denote fold change cut-offs. 88 and 42 T_{reg}-specific genes are upregulated (orange) and downregulated (blue) in fetal naïve T cells. Among T_{reg}-upregulated genes, genes previously associated with T_{reg} function are labeled.

Among T_{reg}-downregulated genes, the top five genes with the lowest p.adj values are labeled.

All boxplots in this figure show median (centre line), interquartile range (box) and tenth and ninetieth percentiles (whiskers).

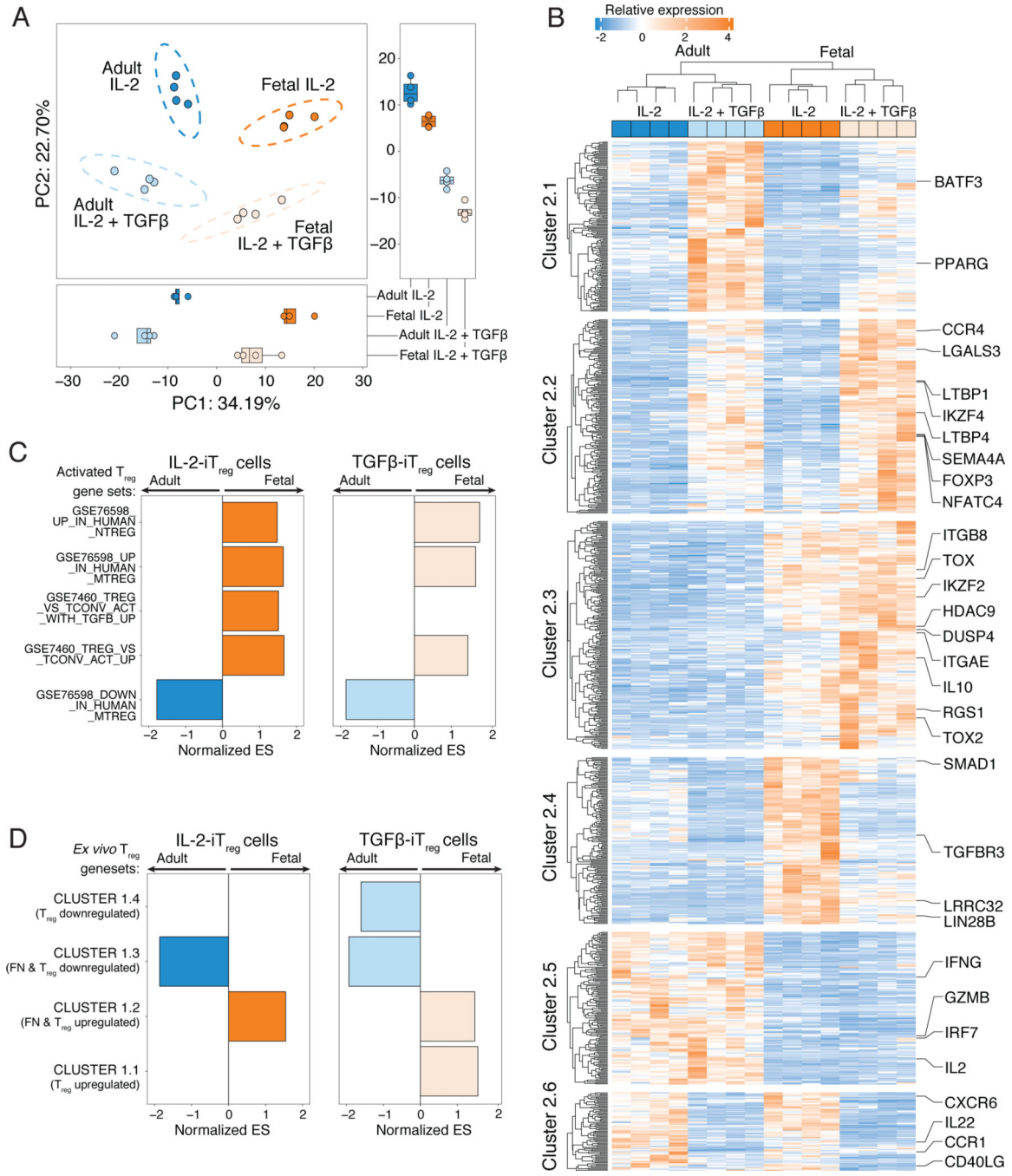

Figure 2. Fetal induced T_{reg} cells retain expression of the partial T_{reg}-specific transcriptome detected in fetal naïve T cells in steady state.

(A) Principal Component Analysis (PCA) of RNAseq data comparing fetal and adult induced T_{reg} cells generated in IL-2 alone (IL-2-iT_{reg}) or with added exogenous TGF-β (TGF-β-iT_{reg}). Boxplots show scores for PC1 (bottom) and PC2 (right).

(B) Heatmap shows relative expression levels of differentially expressed genes (log_2 fold change >1.5, false discovery rate, FDR<0.05) in adult and fetal IL-2- and TGF-β-iT_{reg}

Clusters are labeled and defined by k-means clustering. Genes associated with T_{reg} or pro-inflammatory/effector T cell function are labeled.

(C) Pre-ranked Gene Set Enrichment Analysis (GSEA) was used to assess overrepresentation of pre-defined activated T_{reg}-associated gene sets (see fig. S3B for details of all gene sets) in fetal (orange) or adult iT_{reg} cells (blue) differentiated with IL-2 (left) or IL-2 and TGF-β (right), n=4 for all conditions. Barplot shows normalized Enrichment Scores (ES) for gene sets with FDR<0.05, arrows denote direction of enrichment in adult or fetal iT_{reg} cells.

(D) Pre-ranked GSEA was used to assess overrepresentation of each of the gene clusters identified in Figure 1B. Barplot shows normalized Enrichment Scores (ES) for all clusters with FDR <0.05 for fetal (orange) or adult (blue) iT_{reg} cells differentiated with IL-2 (left) or IL-2 and TGF-β (right).

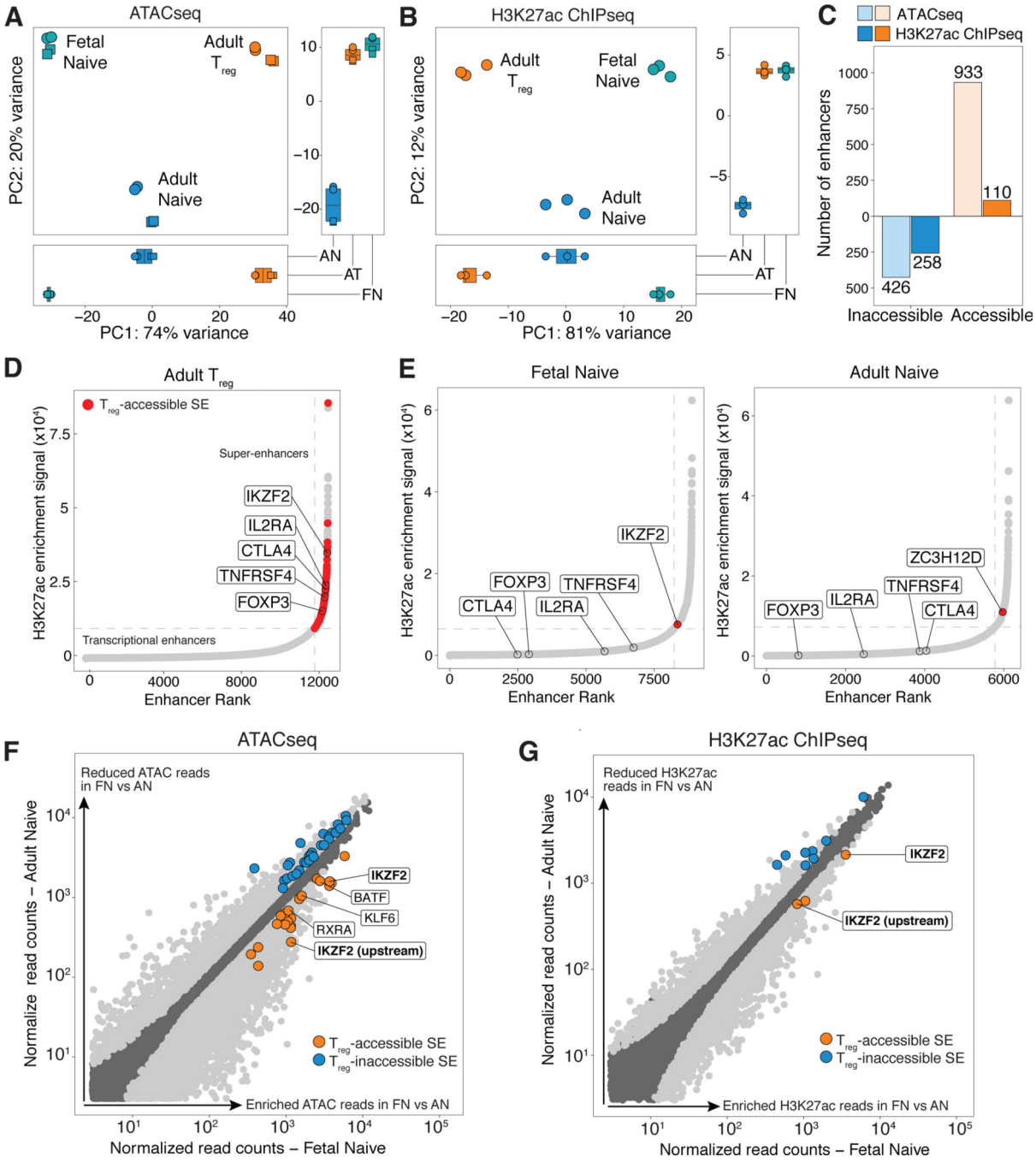

Figure 3. Fetal naïve T cells have increased ATAC and H3K27ac enrichment at two T_{reg}-accessible superenhancers associated with Helios

(A,B) Principal component analysis performed on all super- (SE) and transcriptional enhancers (TE) with mapped **(A)** ATAC or **(B)** H3K27ac reads. Boxplots show scores for PC1 (bottom) and PC2 (right).

(C) Barplots show number of T_{reg}-accessible/inaccessible enhancers with increased (orange) or decreased (blue) ATAC and H3K27ac signal in fetal naïve T cells relative to adult naïve T

cells (T_{reg}-accessible/inaccessible enhancers defined in Supplementary Materials and Methods).

(D) Plots show cumulative H3K27ac signal at stitched enhancers within 12.5kb against enhancer rank, and SEs were defined where the tangent of the plotted curve is 1. Dotted lines (grey) show cutoff for SEs for one representative sample each for adult T_{reg} (n = 3). SEs defined as T_{reg}-accessible and meet fold change (FC) > 1.5 and false discovery rate (FDR) <0.05 cut-offs are colored in red, and SEs associated with key T_{reg} genes are labeled.

(E) Plots as with **(D)** show one representative sample for fetal (left) and adult (right) naïve T cells (n = 3). T_{reg}-accessible SEs identified in **(D)** was assessed for differential enrichment in fetal naïve against adult naïve T cells and vice versa. Differentially enriched T_{reg}-SEs in each sample with FC>1.5 and FDR<0.05 are colored red and labeled. TEs associated with key T_{reg} genes in **(D)** are also labeled.

(F,G) Scatterplots of normalized **(F)** ATACseq reads and **(G)** H3K27ac reads at all stitched enhancer regions of fetal naïve T against adult naïve T cells. Differentially enriched SEs and TEs with FC>1.5 and FDR<0.05 are shown in light grey, with T_{reg}-accessible SEs (orange) and T_{reg}-inaccessible SEs (blue). T_{reg}-accessible SEs associated with transcription factors labeled; Helios (IKZF2) labeled in bold.

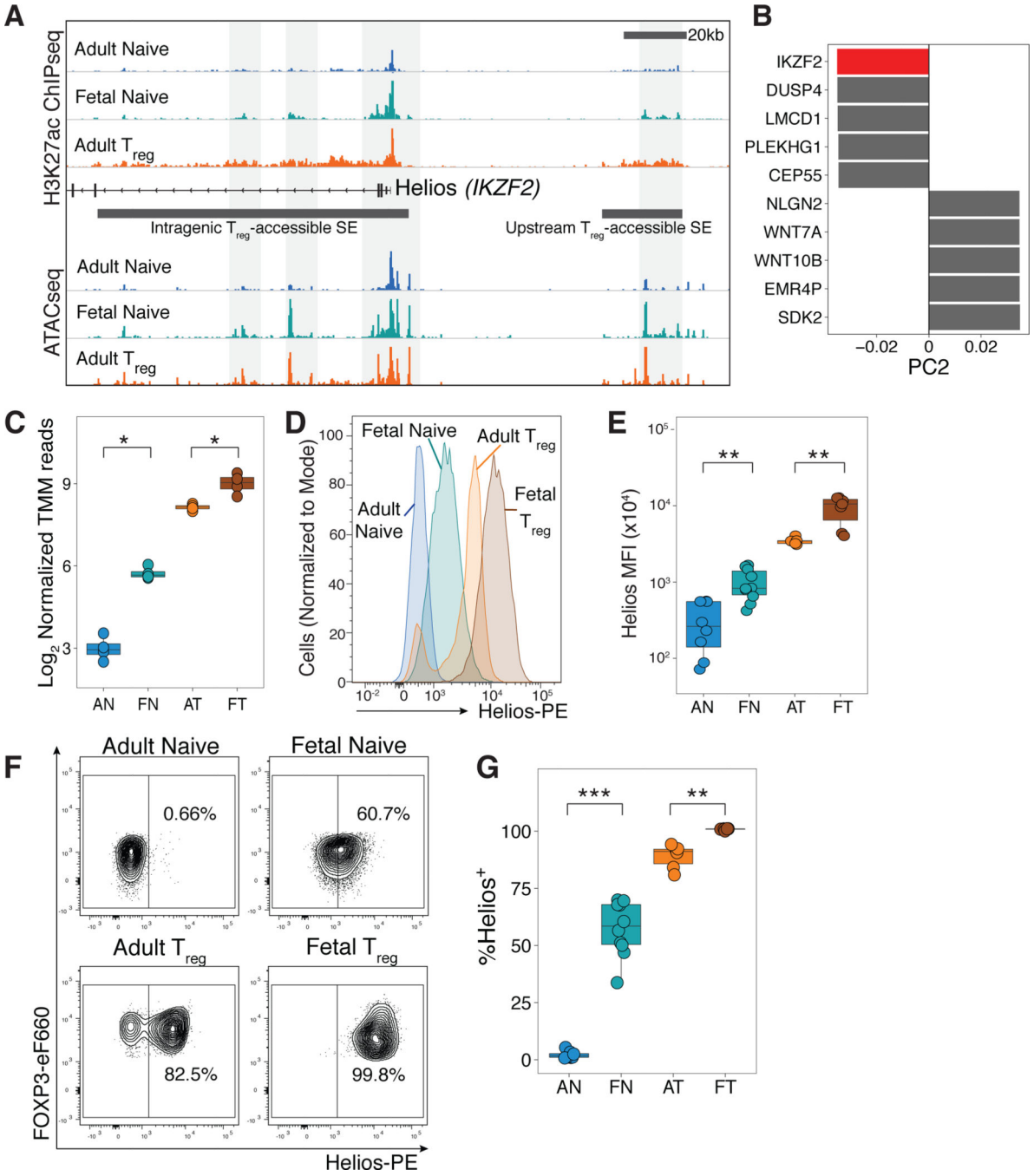

Figure 4. Helios expression is increased in fetal naïve T cells.

(A) Tracks show H3K27ac and ATAC signals at two T_{reg} accessible super-enhancers (SEs) associated with the Helios (IKZF2) locus. Representative tracks of one replicate shown (H3K27ac ChIPseq, n=3, ATACseq, n=2).

(B) The top 5 genes contributing to PC2, which segregates cells by functional subtype (naïve versus T_{reg}) are plotted for both directions; Helios (IKZF2) highlighted in red.

(C) Boxplot shows $\log_2$ trimmed mean of M values of normalized RNAseq reads for Helios in adult naïve (AN), fetal naïve (FN), adult T_{reg} (AT) and fetal T_{reg} (FT) cells (n=4).

(D) Helios staining intensity in sorted $CD4^{+}CD25^{-}CD27^{+}CD45RA^{+}$ adult (blue) and fetal naïve (green), and adult $CD25^{hi}CD127^{lo}FOXP3$ (orange) and fetal T_{reg} (brown).
(E) Boxplot shows quantification of mean fluorescence intensity of Helios for adult naïve (AN, n=8), fetal naïve (FN, n=10), adult T_{reg} (AT, n=8), and fetal T_{reg} (FT, n=10) cells.
(F) Flow cytometry analyses of sorted populations in **(D)**. $Helios^{+}$ and $Helios^{-}$ gates were set based on negative and positive populations in adult T_{reg} samples (bottom left). Adult naïve T cells were universally $Helios^{-}$.
(G) Quantification of $Helios^{+}$ cells among sorted populations in **(F)**.
All statistics were calculated by unpaired two-sided Mann-Whitney test. ***p<0.001, **p<0.01, *p<0.05. All boxplots show median (centre line), interquartile range (box) and tenth and ninetieth percentiles (whiskers)

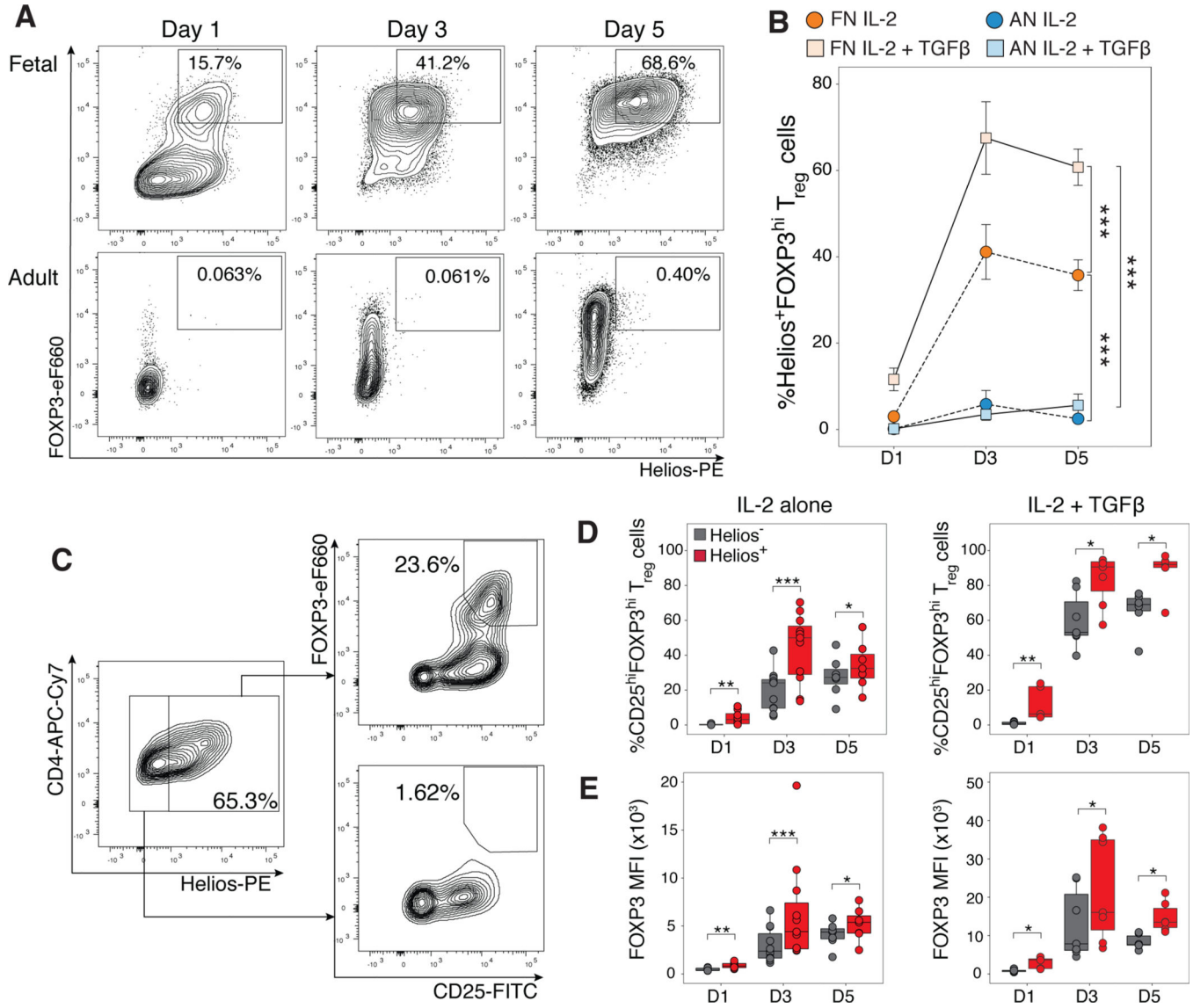

Figure 5. Helios$^+$ fetal induced T_{reg} cells have increased FOXP3 expression

Sorted fetal and adult naïve T cells were stimulated with αCD3/αCD28/αCD2 tetramers and IL-2 in the absence or presence of TGF-β over 1, 3 or 5 days, and analyzed by flow cytometry. The number of biological replicates for each time point and stimulation condition are specified in table S8.

(A) Representative flow cytometry plots show T_{reg} induction in the presence of IL-2 and TGF-β for fetal (top) and adult (bottom) naïve T cells respectively gated on live, CD4$^+$ T cells.

(B) Quantification of percentage of Helios$^+$FOXP3$^+$ iT_{reg} cells gated in **(A)** for adult (AN) and fetal naïve (FN) T cells stimulated in the presence or absence of TGFβ. Statistics calculated using 2-way ANOVA with Tukey's honest significant difference post-test, ***p<0.001. Error bars denote mean ± s.d.

(C) Representative flow cytometry plots shown for one fetal sample stimulated with IL-2 and TGF-β at day 1. **(D)** Quantification of the proportion of fetal T_{reg} cells in the Helios$^+$ or

Helios$^-$ population as gated in **(C)** over 1, 3 and 5 days in the absence (left) or presence (right) of TGF-β.

(E) Quantification of FOXP3 mean fluorescence intensity for Helios$^+$ and Helios$^-$ iT$_{reg}$ cells as gated in **(C)** across all time points in the absence (left) or presence (right) of TGF-β. Statistics for **(D,E)** were calculated by two-sided Wilcoxon signed-rank test, ***p<0.001, **p<0.01, *p<0.05. All boxplots show median (center line), interquartile range (box) and tenth and ninetieth percentiles (whiskers)

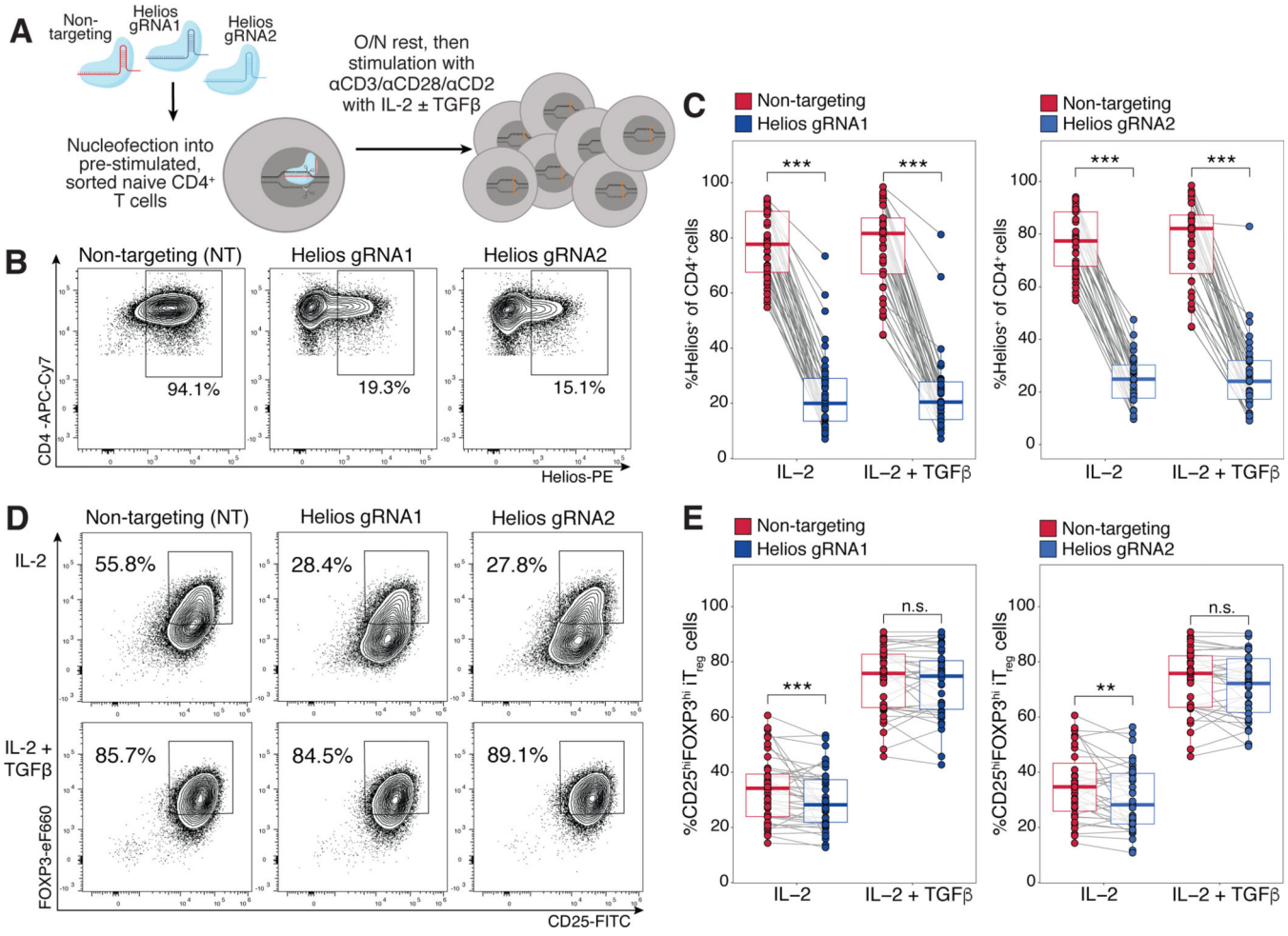

Figure 6. CRISPR-Cas9 mediated knockout of Helios in fetal naïve T cells reduces their preferential differentiation into T_{reg} cells.

A) Schematic showing experimental design. CRISPR-Cas9 editing at the Helios locus with two independent guide RNAs (gRNA1, gRNA2, see Supplementary Materials & Methods) was carried out in pre-stimulated fetal naïve T cells, with a non-targeting (NT) gRNA as a control. Edited cells were stimulated with αCD3/αCD28/αCD2 tetramers in the absence or presence of TGF-β. T_{reg} induction was assessed at 6 days. The numbers of biological replicates for each guide and stimulation condition are specified in table S9.

(B) Flow cytometry plots showing Helios expression in fetal iT_{reg} cells differentiated in IL-2 alone at day 6 after CRISPR-Cas9 editing with Helios gRNA1/2 or NT controls. Representative plots of one experiment are shown gated on live, $CD4^+$ T cells.

(C) Quantification of Helios expression post-editing in fetal naïve T cells after T_{reg} induction as in **(B)**. Boxplots show paired samples for gRNA1 (left) and gRNA2 (right).

(D) Flow cytometry plots showing FOXP3 and CD25 staining in fetal iT_{reg} cells at D6 post CRISPR-Cas9 editing with Helios gRNA1/2 or NT controls. Representative plots of one experiment are shown gated on live, $CD4^+$ T cells.

(E) Quantification of induced T_{reg} proportions in edited fetal naïve T cells as in **(D)**. Boxplots show paired samples for gRNA1 (left) and gRNA2 (right). All statistics were calculated by two-sided Wilcoxon signed-rank test, ***p<0.001, **p<0.01, *p<0.05. All

boxplots show median (center line), interquartile range (box) and tenth and ninetieth percentiles (whiskers).

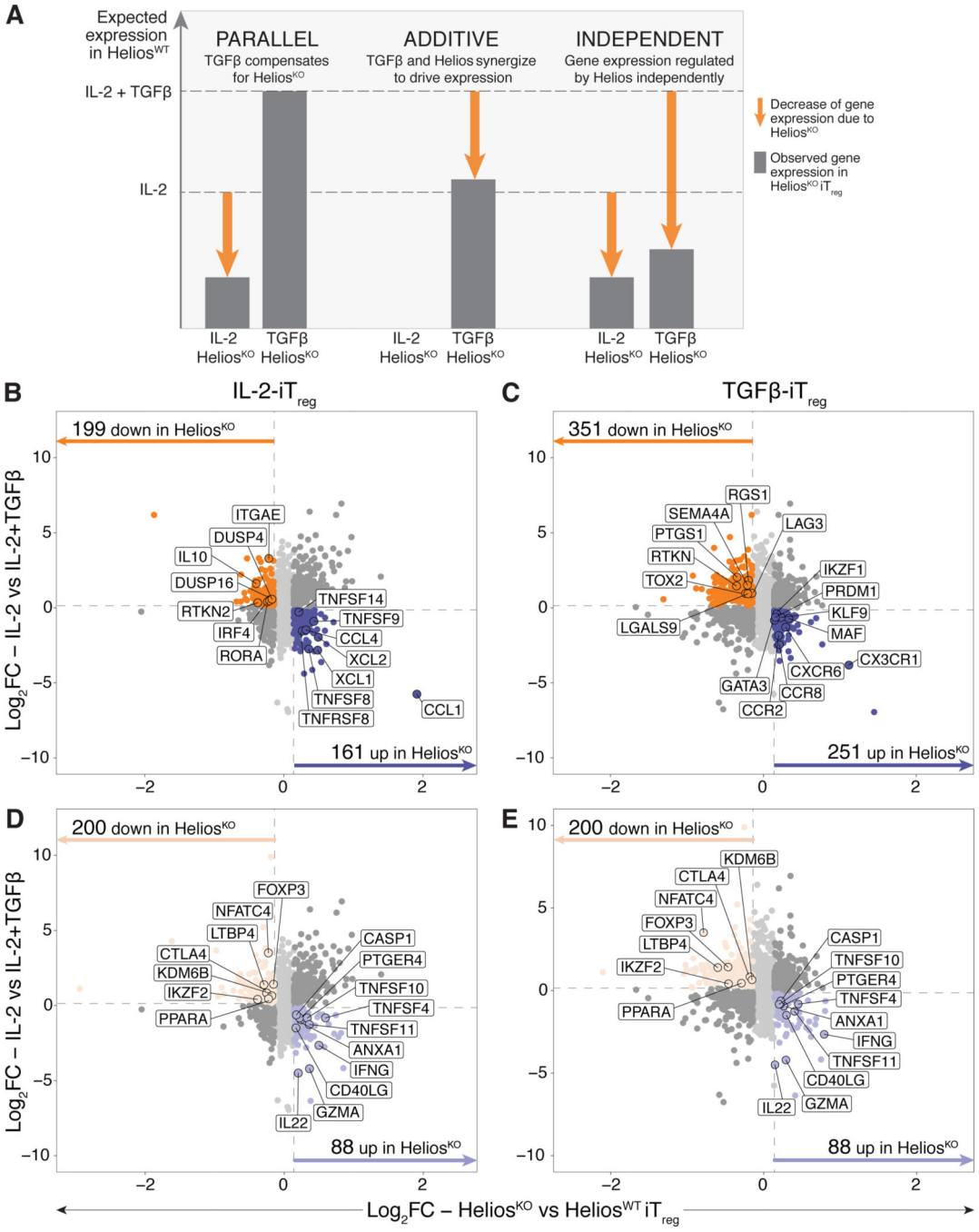

Figure 7. Ablation of Helios in fetal iT$_{reg}$ results in downregulation of T$_{reg}$-specific genes, and the concurrent upregulation of pro-inflammatory genes.

CRISPR-Cas9 editing was carried out in fetal naïve T cells (n=6) with Helios gRNA1 (Helios^{KO}) or the non-targeting control guide (Helios^{WT}). Edited cells stimulated with αCD3/αCD28/αCD2 tetramers in the absence or presence of TGF-β for 6 days, after which changes in their overall transcriptome was assessed by RNAseq.

(A) Schematic showing hypothesized expression levels (dotted lines) of a T$_{reg}$-specific gene that is upregulated with IL-2 in the absence or presence of TGF-β signaling, with proposed

changes in transcription level given one of the three proposed scenarios of transcriptional control by Helios and TGF-β. Gene expression that is driven by Helios is shown, with the arrows denoting the corresponding decrease in gene expression occurring with *Helios* knockout.

(B, C) Scatterplots show log 2 fold change (log_2FC) values comparing the absence or presence of exogenous TGFβ during the differentiation process (y-axis) and $Helios^{KO}$ against $Helios^{WT}$ iTreg (x-axis) that underwent differentiation in IL-2 alone **(B)** or with exogenous TGF-β added **(C)**. Dotted lines in grey denote log_2FC cut-offs. Only genes upregulated (dark purple) or downregulated (dark orange) in $Helios^{KO}$ relative to $Helios^{WT}$ iT_{reg} cells are colored and shown (fold change, FC>1.1, false discovery rate, FDR<0.05). Genes associated with T_{reg} or pro-inflammatory immune functions are outlined and labeled.

(D, E) Same scatterplots as in **(B,C)** for IL-2 only iT_{reg} cells **(D)** and IL-2 + TGF-β-iT_{reg} **(E)** now colored to only show shared genes meeting the same cutoffs that were upregulated (light purple) or downregulated (light orange) in $Helios^{KO}$ relative to $Helios^{WT}$ iT_{reg} cells. Genes associated with T_{reg} or pro-inflammatory immune functions within the shared Helios-regulated transcriptome are outlined and labeled.

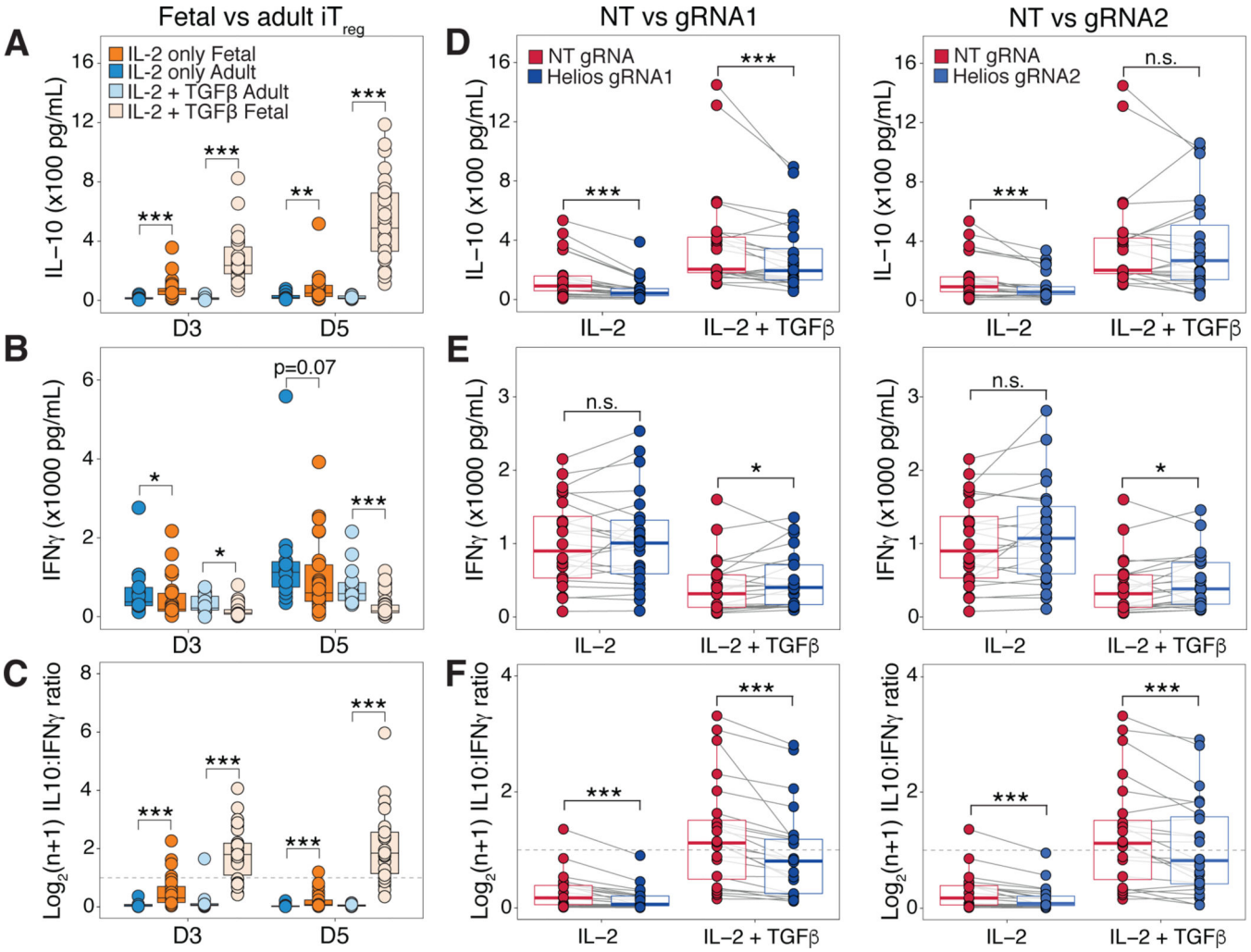

Figure 8. Fetal Helios knockout iT$_{reg}$ cells have decreased IL-10 and increased IFN-γ cytokine production.

A) Boxplots quantify IL-10 cytokine concentration within culture supernatants collected at day 3 and 5 of differentiation for adult (blue, n=27) or fetal iT$_{reg}$ cells (orange, n=58) differentiated in IL-2 alone (IL-2 iT$_{reg}$), as well as adult (light blue, n=27) or fetal (light orange, n=55) iT$_{reg}$ cells differentiated with added TGF-β (TGF-β-iT$_{reg}$).

(B) Boxplots quantify IFN-γ cytokine concentrations for samples as in **(A)**.

(C) Boxplots show log$_2$(n+1) ratio of IL-10 to IFN-γ cytokine concentration for samples as in **(A)**. Dotted line marks the ratio at which cells produce IL-10 and IFN-γ at 1:1. All statistics for **(A,B,C)** calculated by unpaired two-sided Mann-Whitney test,*** p<0.001, ** p<0.01, *p<0.05.

(D) Boxplots quantify IL-10 cytokine concentrations at day 5 of differentiation for iT$_{reg}$ cells that received the non-targeting guide (Helios^{WT}, red) or for Helios knockout (Helios^{KO}, blue) with gRNA1 (left, n=24) and gRNA2 (right, n=23).

(E) Boxplots quantify IFN-γ cytokine concentrations for samples in **(D)**.

(F) Boxplots show log$_2$(n+1) ratio of IL-10 to IFN-γ cytokine concentration for samples as in **(D)**. Dotted line marks the ratio where cells produce IL-10 and IFN-γ at 1:1. All statistics

for **(D,E,F)** calculated by two-sided Wilcoxon signed-rank test, *** $p<0.001$, * $p<0.05$, n.s. $p>0.05$. All boxplots show median (center line), interquartile range (box) and tenth and ninetieth percentiles (whiskers).